RECORDING AND ANALYSIS OF ATOMIC SPECTRA IN VACUUM ULTRAVIOLET REGION

DISSERTATION

SUBMITTED IN THE PARTIAL FULFILLMENT OF THE REQUIREMENT FOR THE AWARD OF THE DEGREE OF

Master of Philosophy

In

Physics

By

Sumit Mishra

Under the supervision of

Prof. Rahimullah Khan

Department of Physics
Aligarh Muslim University
Aligarh (UP)-202002, INDIA
2011

Dedicated

To

My

Loving

Parents

DEPARTMENT OF PHYSICS

ALIGARH MUSLIM UNIVERSITY

ALIGARH- 202002.

Certificate

This is to certify that the work presented in the dissertation entitled **"Recording and Analysis of Atomic Spectra in Vacuum Ultra-Violet Region"** submitted by Mr. Sumit Mishra, in partial fulfillment of the requirements for the award of the degree of Master of Philosophy in Physics is based on the work done by him under my supervision.

Prof. Rahimullah Khan

ACKNOWLEDGEMENT

ALL MY PRAISES TO **GOD**, FOR SHOWERING HIS BLESSINGS UPON **ME** FOR MAKING ME ABLE TO COMPLETE THIS PIECE OF WORK.

BEGINNING WITH DEEP GRATITUDE TO MY HONORABLE SUPERVISOR **PROF. RAHIMULLAH KHAN**, FOR HIS NOBLE GUIDANCE AND CONSISTENT ENCOURAGEMENT TO ACCOMPLISH THIS TASK.

IT IS PLEASURE TO OFFER MY SINCERE THANKS TO **PROF. TAUHEED AHMAD** FOR HIS HELP.

MY SINCERE THANKS ARE DUE TO **PROF. WASI HAIDER**, CHAIRMAN, DEPARTMENT OF PHYSICS, AMU, ALIGARH FOR PROVIDING THE WORK FACILITIES.

I AM ALSO BEHOLDEN TO **MR. RAHIMUDDIN** WHO SUPPORTED ME THROUGHOUT MY WORK. THANKS ARE ALSO DUE TO **MR. MOHANLAL** FOR HIS SUPPORT AND COOPERATION.

I WOULD ALSO LIKE TO THANK MR. MANOJ KUMAR, MR. RIYAZ AHEMAD AND MR. HARIS KUNARI FOR ENCOURAGEMENT TO ACCOMPLISH THIS TASK.

I AM HIGHLY DELIGHTFUL IN PAYING DEEP SENSE OF GRATITUDE TO MY FRIENDS, MR. ABHISHEK YADAV, MR. KAMAL KUMAR, MR. HARISH KUMAR, MR. VIJAY RAJ AND MR. MUNISH KUMAR AND ALL OTHERS WHO MORALLY SUPPORTED ME DURING MY WORK.

DO NOT HAVE WORDS TO EXPRESS MY GRATITUDE TO MY PARENTS, BROTHERS SUNIL AND SACHIN FOR THEIR MORAL SUPPORT IN MY LIFE.

Sumit Mishra

SUMIT MISHRA

CONTENTS

Chapter-1

Introduction

Atomic emission spectroscopy relates to electronic transitions in atoms which uses an excitation source like flame, arc or spark and argon plasma source etc. Most of the spectroscopic techniques are related to molecules but emission spectroscopy is related to atoms. Radiation is produced when atoms are excited. They emit radiations in the form of discrete wavelengths of light, called spectral lines while returning to the lower energy states. The wavelength of a spectral line is inversely proportional to the energy difference between the initial and final energy levels. Since no two elements have identical energy levels hence the same spectra.

In 1893, Schumann built the first spectrograph suitable for investigating the region beyond 2100 Å. The region was named the Schumann region, after its discoverer, and is also called the vacuum ultraviolet (VUV). It is located between about 2100 Å and the limit of soft x rays (~10 Å).The delay in investigating this region was due to the atmospheric oxygen which absorbs nearly all radiations beyond 2100 Å .[1]

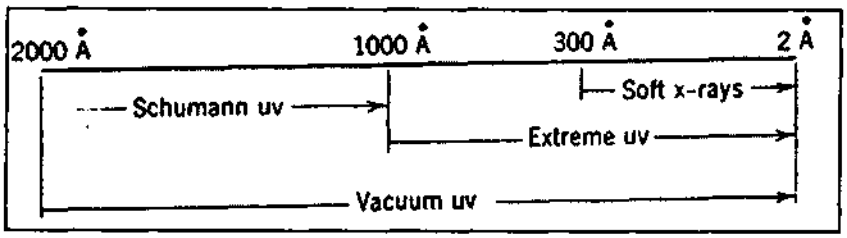

The study of both emission and absorption of radiations in this region has not been utilized much until relatively recently for several reasons. The first of these is probably that, until a few decades ago, practically no spectroscopic apparatus for this region was commercially available. Anyone who desired to carry out research in this field had to build his own apparatus. Today the situation is completely changed, and many good instruments built in Belgium, Britain, Canada, China, France, Germany, Italy, Japan, U.K. and the United States are now commercially available.

Difficulties encountered in vacuum ultra-violet spectroscopy can arise from

a) Absorption of the radiations by the optical materials;
b) Light sources;
c) Detectors;
d) The necessity of working with gases or vapours.

The difficulty with atmospheric gases could be overcome by filling the optical path with some transparent gas; but it is better to eliminate all atmospheric gases, in particular oxygen, from the optical path. Absorption of radiations by oxygen begins to be noticeable at wavelengths slightly greater than 2000 Å (with the system of Schumann-Runge bands), and its intensity increases rapidly towards the shorter wavelengths. The different electronic transitions of oxygen give rise to many other absorption regions so that, in the presence of oxygen, the only portion of the Schumann region which is at all usable lies between 1100 and 1200 Å.

The second major component of the atmosphere, nitrogen, is almost transparent down to about 1000 Å. Below this wavelength, the absorption increases, and becomes very intense below 850 Å. Other minor atmospheric components (water vapour, carbon dioxide, rare gases, etc.) are present at such low partial pressures, especially after evacuation, that they may be neglected.[2]

I have chosen to study Zinc spectra in the vacuum ultra-violet region. Zinc (German: Zink), also known as spelter, is a metallic chemical element; it has the symbol **Zn** and atomic number 30. Zinc is a bluish-white, lustrous, diamagnetic metal. In chapters 2, 3 and 4; Hartree-Fock approximations, light sources and grating spectrographs respectively, have been described. Chapters 5 and 6 deal with our vacuum spectrograph and vacuum techniques. The last two chapters 7 and 8 are devoted to discuss the details of the recording, measurements and the structures of Zinc.

Chapter-2

Theoretical Aspect

The emission of spectra from atoms could not be explained by Thomson's model of atom. After that Rutherford's model of atom came into account that was unable to explain the line spectrum and stability of the atom. Bohr removed these difficulties of Rutherford's atomic model by the application of Planck's quantum theory.

Bohr's model explains the spectra of one-electron atoms only such as hydrogen, hydrogen isotopes, singly-ionized helium, and doubly-ionized lithium, etc. It fails to explain the spectra of multi-electron atoms. After that the quantum mechanical treatment of the atom came into account.

We know that Schrodinger's equation cannot be solved exactly for two electron atoms or ions, so that some approximation methods are used. We can use some variational methods for calculating the energy levels and wave functions of helium-like atoms. In variational approach we choose a trial wave function which contains large number of variational parameters. This approach cannot be applied to study the structure of multi-electron atoms or ions. So we used another approximation.

The Central field approximation began in early 1920's. In this each electron moves in a central field, created by the nucleus and the spherically averaged potential field of each other electron. We take strong attractive Coulomb force between nucleus and electrons, and a comparatively small repulsive force between electrons.

In this approximation spin of electrons are not considered. It explains the spectrum of neutral alkali atom very well but not the atoms having complex multiplet structures.

In 1928, Hartree gave a theory of self consistent field. He modified the central field problem for the presence of extra nuclear electrons. In this method, a total wave function

is considered as a product of all the individual electron wave functions involved in the system, which is symmetric and do not follow the Pauli's exclusion principle.

In 1930, the theory was again modified by Fock. He introduced the antisymmetric wave function to the formulae; the method was known as Hartree-Fock method. He used a determinantal function or a linear combination of determinantal functions to satisfy the conditions of antisymmetry.

A total N-electron (Central field) wave function $\Psi_c(q_1,q_2,....,q_N)$ which is antisymmetric in the (spatial and spin) coordinates of any two electrons is used, in order to satisfy the condition of Pauli's exclusion principle. The total wave function ψ_c describing an atom in which one electron is in state α , another in state β , and so on may be written as a N×N determinant,

$$\Psi_c(q_1,q_2,....,q_N)=\frac{1}{\sqrt{N!}}\begin{vmatrix} u_\alpha(q_1) & u_\beta(q_1) & \cdots & u_\nu(q_1) \\ u_\alpha(q_2) & u_\beta(q_2) & \cdots & u_\nu(q_2) \\ \vdots & & & \\ u_\alpha(q_N) & u_\beta(q_N) & \cdots & u_\nu(q_N) \end{vmatrix}$$

This is known as Slater determinant. This wave function is obviously antisymmetric because if we interchange the spatial and spin coordinates of two electrons this is equivalent to interchanging two rows, the determinant changes sign. We also know that a determinant vanishes when two columns or rows are equal, so the Slater determinant will vanish if two electrons have the same values of all the four quantum numbers n , l , m_l , m_s .[3]

(2.1) Hartree-Fock Approximation :

The Hamilton operator consists of two parts:

$$H = H_0 + H_{ee}$$

The first term is given by

$$H_0 = \sum_j \left[\frac{p_j^2}{2m_e} + V\left(r_j\right) \right]$$

Where m_e is the electron mass and V is the potential energy of an electron in the electric field of the atomic nucleus. The momentum operator is $\vec{p} = -i\hbar\vec{\nabla}$ according to the correspondence principle. The sum goes over all electrons of the atom.

The second term of the Hamilton operator represents the Coulomb interaction between the electrons

$$H_{ee} = \frac{1}{2}\sum_{i \neq j} \frac{e^2}{\left|r_i - r_j\right|}$$

For atoms containing more than one electron, the time-independent Schrödinger equation can only be solved by approximate methods because of the interaction term H_{ee}.

The Hartree-Fock approximation assumes that each electron moves in an effective centrally symmetric potential created by the nucleus and all other electrons. This takes care of the screening of the potential V, as seen by a certain electron, due to the mean field of the other electrons. The screening depends itself on the orbitals of the electrons. This treatment of the screening is known as self consistent field method introduced by Hartree. Within this approximation the total wave function has the form of a product of the individual electron orbitals. Thus, each electron is supposed to occupy its own orbital while the state of the atom as a whole is determined by the set of electronic states. However, the Hartree-Fock approximation goes even a step further and properly treats the Pauli principle by ensuring that the total wave function is antisymmetric with respect to the exchange of electrons as is satisfied by the Slater determinant.[4]

(2.2) Cowan Code :

The Schrodinger equation can be solved only for the hydrogen atom. The structures of complex atoms where many electrons are involved, is not simple. So it is impossible to

find the solution of the Schrodinger's equation for complicated structures. R. D. Cowan developed a computer code to solve these complicated equations. Cowan code is a suite of four programs (RCN, RCN2, RCG and RCE) that calculates atomic structures and spectra.

1. **RCN:** Primary information is given to RCN. For this we provide input files IN2 and IN36. It calculates one-electron radial wave functions (bound or free) for each of any number of specified electron configurations, using the Hartree-Fock or any of several more approximate methods. The principal output, for each configuration, consists of the center-of-gravity energy (E_{av}) of the configuration, and those radial Coulomb (F^k and G^k) and spin-orbit (ζ) integrals required to calculate the energy levels for that configuration. The input file IN36 for RCN program of Zinc atom (doubly ionized) to run Cowan Code is shown below.

```
200-90 0 2  01.  0.2    5.E-08    1.E-11-2 00190 0 1.0  0.65  0.0 1.00   -6
   30    3Zn3   3d10      3P6  3D10
   30    3Zn3   4s1       3P6  3D9  4S1
   30    3Zn3   5s1       3P6  3D9  5S1
   30    3Zn3   6s1       3P6  3D9  6S1
   30    3Zn3   7s1       3P6  3D9  7S1
   30    3Zn3   8s1       3P6  3D9  8S1
   30    3Zn3   9s1       3P6  3D9  9S1
   30    3Zn3   d94d      3P6  3D9  4D1
   30    3Zn3   d95d      3P6  3D9  5D1
   30    3Zn3   d96d      3P6  3D9  6D1
   30    3Zn3   d95g      3P6  3D9  5G1
   30    3Zn3   d96g      3P6  3D9  6G1
   30    3Zn3   d97g      3P6  3D9  7G1
   30    3Zn3   d98g      3P6  3D9  8G1
   30    3Zn3   3d84s2    3P6  3D8  4S2
   30    3Zn3   4p1       3P6  3D9  4P1
   30    3Zn3   5p1       3P6  3D9  5P1
   30    3Zn3   6p1       3P6  3D9  6P1
   30    3Zn3   4f1       3P6  3D9  4F1
   30    3Zn3   5f1       3P6  3D9  5F1
   30    3Zn3   3d84sp    3P6  3D8  4S1  4P1
   -1
```

2. **RCN2:** It uses the output radial wave-functions from RCN that becomes the input to RCN2. It calculates the configuration-interaction Coulomb integrals (R^k) between each pair of interacting configurations, and the electric dipole (E^1) and/or electric quadrupole

(E^2) radial integrals between each pair of configurations. RCN2 prepares an output file. It becomes input file for RCG.

3. **RCG:** It computes energy matrices for each possible value of the total angular momentum J, diagonalizes each matrix to get eigenvalues (energy levels) and eigenvectors and then computes M^1 (magnetic dipole), E^2 , and/or E^1 radiation spectra, with wavelengths, oscillator strengths, radiative transition probabilities, and radiative lifetimes.

4. **RCE:** It is a least squares fitting program. When sufficient number of levels (say about 50%) are experimentally known, then these levels are used as an input for RCE program to recalculate the Slater Parameters (E_{av}, F^k, G^k, ζ, and R^k) by making them free and adjust themselves.[5]

Chapter-3

Light Sources

Light sources, or sources of radiant energy, may be classified according to the method used for exciting radiation, the type of spectrum emitted, the spectral region to which the source is best adapted (infrared, visible, ultraviolet, or extreme ultraviolet).
There are some main sources (which are used widely):

- Thermal radiators,
- Arc sources,
- Discharge tubes,
- Spark sources;
- Lasers.

Now we will discuss electric arcs and electric sparks as we used spark source in our experiment.

(3.1) Electric Arcs :

An electric arc is a simple set of two solid electrodes. An insulating holder is required for the electrodes, a direct-current source of 100 or more volts, and a ballast resistance. The ballast resistance is necessary because the voltage across an arc depends little on the current but almost wholly on the nature of the electrodes, the pressure and character of the surrounding gas, and the length of the arc. The voltage-current characteristics is exceedingly steep and may even have a negative slope in some regions, so that, without a ballast resistance, the current is unstable and may increase without limit until a fuse or circuit burns out.

The excitation of the atoms or molecules in the arc column is pure thermal, with temperature of 3500-8000 ^{0}C. Arcs are operated in another atmosphere too as nitrogen, hydrogen, helium or argon. The arc in most of these gases gives a higher temperature or

excitation than the arc in air. Arcs may also be operated at reduced pressure and in this case, lines are produced that are of much higher excitation, as well as sharper, and are free from the small line displacements caused by pressure effects.

The arc has many advantages: it is cheap and simple to set up and can be used with any kind of conducting electrodes. Scarce materials, non conducting elements, or salts can be packed in holes drilled in the tips of graphite electrodes; solutions can be dried on the tips of graphite or copper electrodes. [6]

(3.2) Electric Sparks :

We have used spark source in our experiment. It produces higher excitation/ionization. The spark is produced by connecting the secondary of a transformer giving from 10,000 to 50,000 volts across an insulated electrode-holder which carries the test samples. The high potential gradient set up across the spark gap by this voltage pulls from the negative electrode a cold emission of electrons, which is largely responsible for initiating discharge. A condenser is connected in parallel across the secondary. The effect of the condenser is to increase the discharge current across the gap.

The condenser is charged on every half-cycle to the voltage at which the gap breaks down. An oscillatory discharge current then flows in the spark circuit with an initial value given by

$$I = V \sqrt{\frac{C}{L}}$$

Where, V is the condenser voltage at the time of discharge, C the capacity in Farad, and L the circuit inductance in Henry. The initial current may be hundreds of amperes. The result is an almost explosive emission of excited vaporized material from the electrodes. A small amount of inductance is desirable in the spark circuit, since it has been found to prevent the excitation of lines and bands of the air molecules which otherwise cause undesirable confusion and background in the spectrum. Larger amounts of inductance decrease the initial current and degree of excitation/ionization in the spark.

With the sparks, any conducting solid electrodes may be used directly. Substances which are rare, non conducting, powdered, or otherwise unsuitable for use as solid electrodes

may be packed in a hollow carbon or aluminum electrode, alloyed with other material, or pressed or sintered with metal powders into a solid electrode. [6]

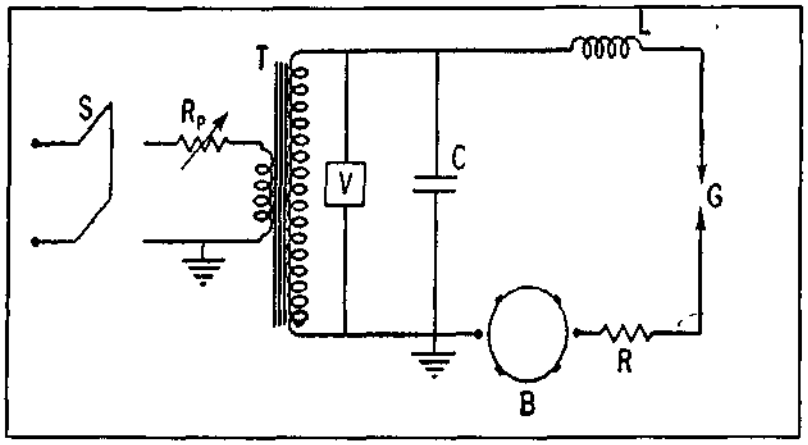

Figure (3.1): Controlled spark circuit. S, primary switch; R_p, primary resistance; T, high-voltage transformer; V, electrostatic voltmeter; C, capacitance; L, inductance; B, synchronous rotating spark gap; R, damping resistance; G, spark gap for sample.

(3.3) Construction of Spark Chamber and Power Supply :

The D.C. Spark Source used in our experiment was designed in the Workshop of physics department A.M.U. Aligarh. The spark chamber was constructed by using thick Perspex sheets. Three square shapes Perspex sheets of dimension 4×4 inches are taken and each sheet has a thickness of the order of 16 mm. Perspex sheets are joined together through rubber O-rings to prevent the leakage from the chamber. In every sheet there are four holes to fit the bolts. The middle sheet was cut in centre (of diameter two inches) for the space of electrodes. The components of this spark source are high voltage power supply, inductor coil, capacitor, diodes and Cu, Zn electrodes.

The power supply of variable d.c. output up to 12500 V was used. The Inductor coil of 5 turns with Copper wire was wound on a cylindrical wooden block of diameter 6.5 inch. One end of coil is connected to the Capacitor and the other end is so chosen to vary the number of turns. This coil, used to provide necessary current density, was connected across a capacitor and electrodes as shown in Figure (3.3). The inductance can be purposefully introduced in series with the source to select unknown spectral lines since radiation from the higher stages of ionized atoms disappears first as series inductor is

increased. A very low inductance leads to production of radiation from a very high stage of ionization.

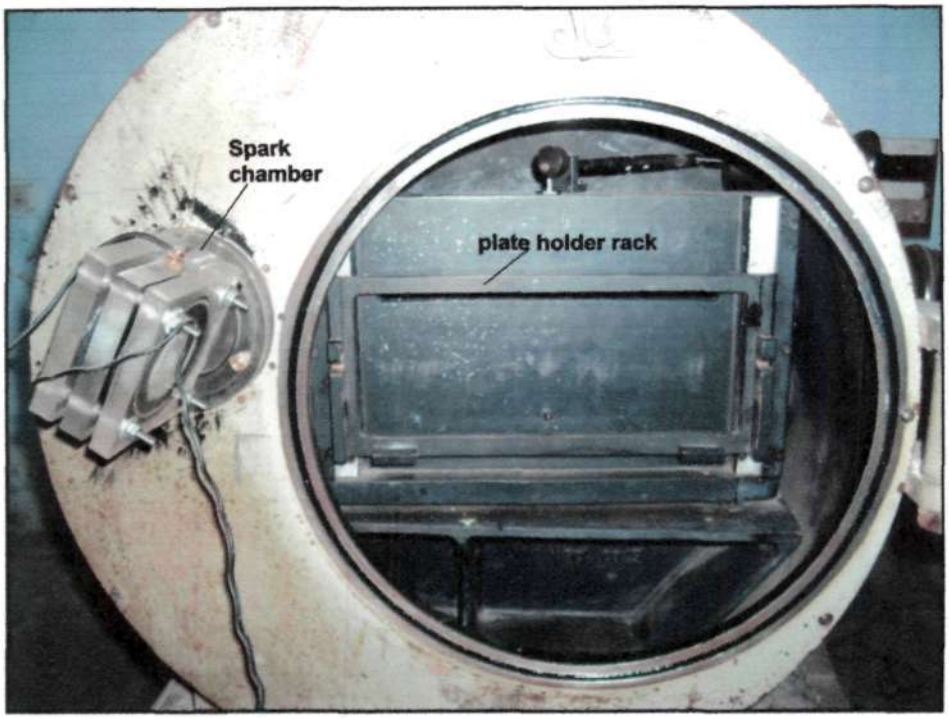

Figure (3.2): Spark Chamber is fitted with 3-metre vacuum spectrograph

Dimmerstat continuously variable autotransformer	0-260 V
Foster Transformers L.T.D. LONDON S.W.19. ENGLAND (Made to the specification of Hilger & Watts)	8 KV
Diodes (connected in series, Quantity in numbers)	12
Pyrandol Capacitor (DC 12500 V)	3.21 μF
Inductor coil (number of turns)	5
Inductance (Quantity in number)	I

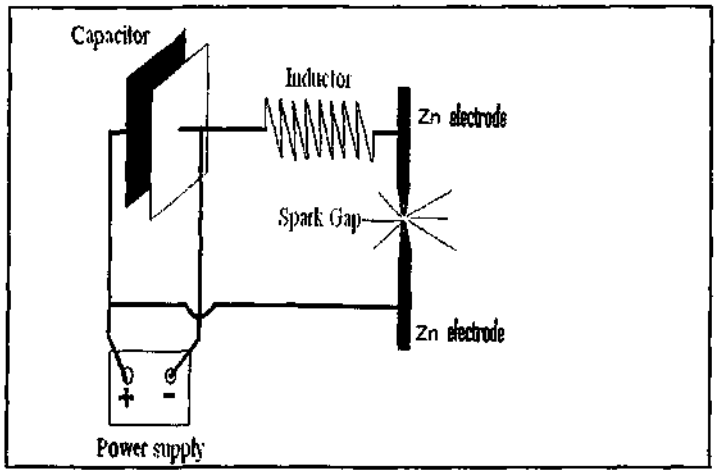

Figure (3.3): Spark Source

The spark discharge sources are of the following two types:

- Sliding spark discharge
- Open spark discharge

(3.4) Sliding Spark Discharge :

Vacuum spark discharge was first used by Millikan to study the spectra of metals in the extreme ultraviolet. In this spark discharge, the electrons are rapidly worn away and the sputtered material clogs the spectrograph slit.

Vodar and Astoin designed a high vacuum spark discharge called "Sliding Spark Discharge". In this spark discharge; the electrodes were separated by, an insulator (which was in good contact with the electrodes). The spark discharge occurred on the surface of the insulator (quartz, porcelain, or alumina). It could be produced at lower voltages and with less sputtering of electrode material. The radiation emitted was characteristics of the metal of the electrodes and also of the insulating material. The separation of the electrodes can be much greater in the sliding spark discharge than with the Millikan source.[7]

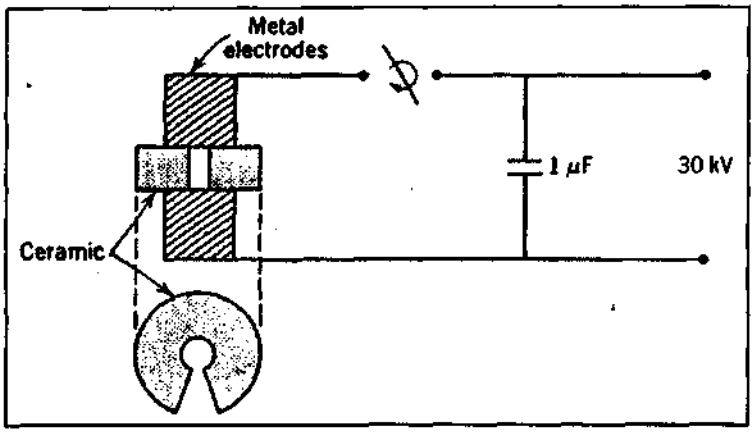

Figure (3.4): Arrangement of the electrodes and insulator in the sliding spark light source.

(3.5) Open Spark Discharge :

In our experiment we have used a open spark discharge source. It produces relatively higher excitation/ionization. It is same as the sliding spark discharge, except only one difference, that there is no insulator between the gap of electrodes.

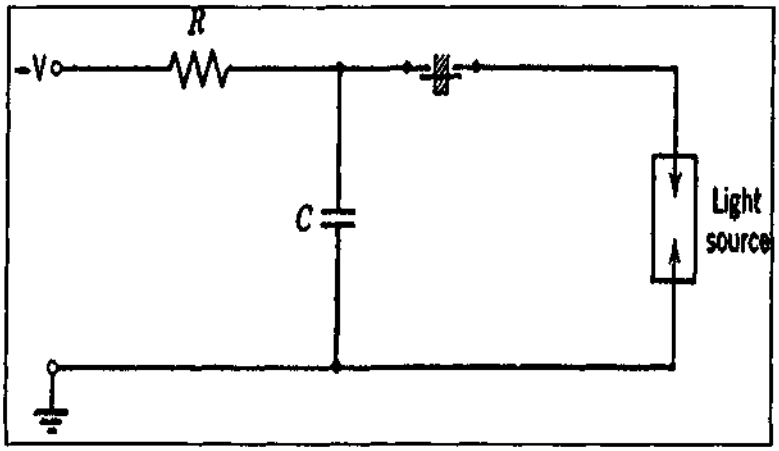

Figure (3.5): Open spark discharge

Chapter-4

Spectrograph

A spectroscope is an instrument which separates different wavelengths, i.e., disperses them into a spectrum for visual observation. A spectrograph is an instrument for producing a spectrogram, a photographic image of the spectrum.

The spectrograph consists of:

1) A dispersing device which gives to different wavelengths passing through it different emergent angles;
2) An optical system of mirrors or lenses to bring the various wavelengths to various foci in a focal plane;
3) An entrance aperture, usually a rectangular slit, whose images, formed by the optical system in radiation of different wavelengths, are the spectral "lines" which are observed or photographed.[6]

Types of spectrographs:

- Prism spectrograph,
- Grating spectrograph.

In our experiment we used a grating spectrograph that requires the knowledge of following informations.

(4.1) The Grating Equation :

When monochromatic light is incident on a grating surface, it is diffracted into discrete directions. We can picture each grating groove as being a very small, slit-shaped source of diffracted light. The light diffracted by each groove combines to form set of diffracted wavefronts. The usefulness of a grating depends on the fact that there exists a unique set of discrete angles along which, for a given spacing d between grooves, the diffracted light from each facet is in phase with the light diffracted from any other facet, leading to constructive interference. Diffraction by a grating can be visualized from the geometry in Figure 4.1, which shows a light ray of wavelength λ incident at an angle α and

diffracted by a grating (of groove spacing d, also called the pitch) along at set of angles $\{\beta_m\}$.

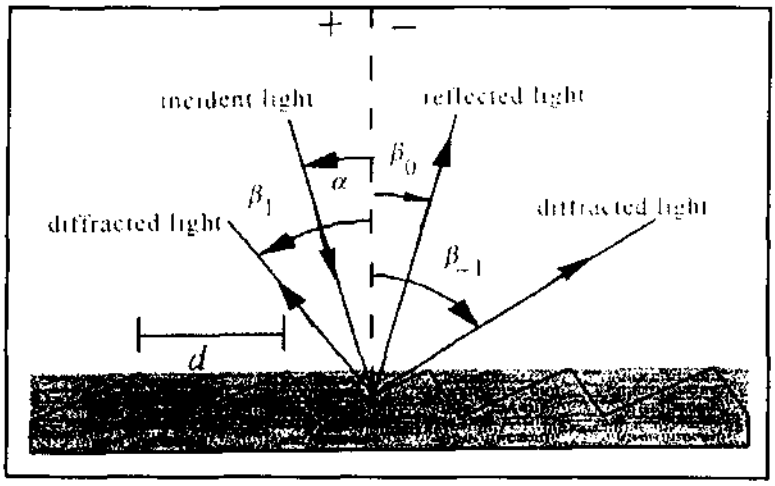

Figure (4.1a): A reflection grating: the incident and diffracted rays lie on the same side of the grating.

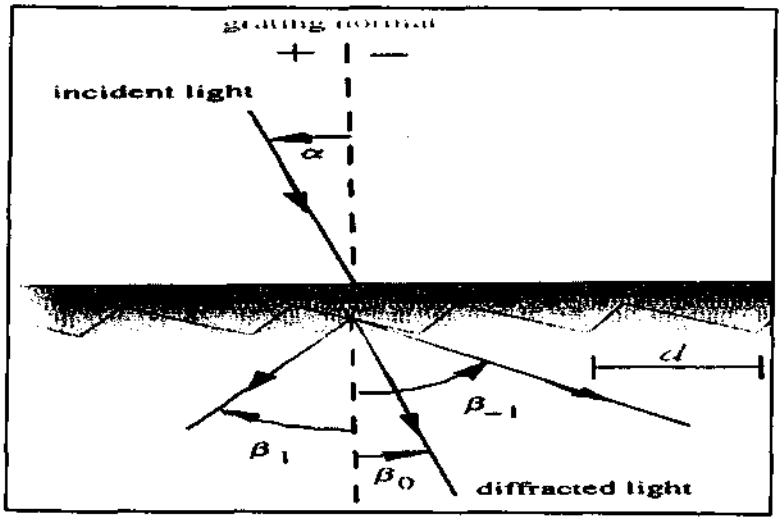

Figure (4.1b): A transmission grating: the diffracted rays lie on the opposite side of the grating.

The β_m angles are measured from the grating normal, which is shown as the dashed line perpendicular to the grating surface at its center. The sign convention for these angles depends on whether the light is diffracted on the same side or the opposite side of the grating as the incident light.

Figure (4.1a) shows a reflection grating, the angles $\alpha > 0$ and $\beta_1 > 0$ (since they are measured counter-clockwise from the grating normal) while the angles $\beta_0 < 0$ and $\beta_{-1} < 0$ (since they are measured clockwise from the grating normal).

Figure (4.1b) shows the case for a transmission grating. By convention, angles of incidence and diffraction are measured from the grating normal to the beam. This is shown by arrows in the diagrams. In both diagrams, the sign convention for angles is shown by the plus and minus symbols located on either side of the grating normal. For either reflection or transmission gratings, the algebraic signs of two angles differ if they are measured from opposite sides of the grating normal. Other sign conventions exist, so care must be taken in calculations to ensure that results are self-consistent. Another illustration of grating diffraction, using wavefronts (surfaces of constant phase), is shown below.

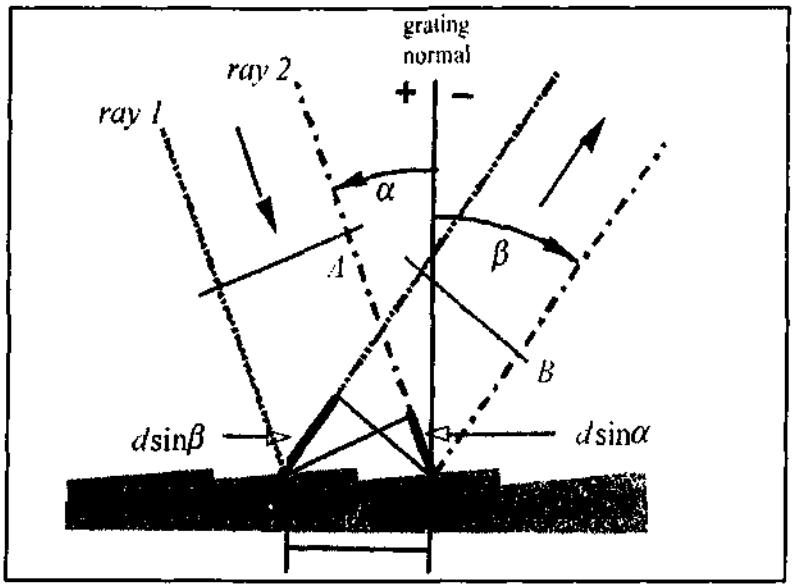

Figure (4.2): Geometry of diffraction, for planar wavefronts.

Two parallel rays, labeled 1 and *2*, are incident on the grating one groove spacing *d* apart and are in phase with each other at wavefront *A*. Upon diffraction, the principle of constructive interference implies that these rays are in phase at diffracted wavefront *B* if the difference in their path lengths, (d $\sin\alpha$ +d $\sin\beta$), is an integral number of wavelengths; this in turn leads to the grating equation.

$$m\lambda = d\sin\alpha + d\sin\beta \quad (4.1)$$

Here m is the diffraction order (or spectral order), which is an integer. It is sometimes convenient to write the grating equation as

$$Gm\lambda = \sin\alpha + \sin\beta \quad (4.2)$$

Where $G = 1/d$ is the groove frequency or groove density, more commonly called "grooves per millimeter".[8]

(4.2) Diffraction Orders :

Generally several integers m will satisfy the grating equation – we call each of these values a diffraction order. For a particular groove spacing d, wavelength λ and incidence angle α, the grating equation (4.1) is generally satisfied by more than one diffraction angle β.

There will be several discrete angles at which the condition for constructive interference is satisfied. The physical significance of this is that the constructive reinforcement of wavelets diffracted by successive grooves merely requires that each ray be retarded (or advanced) in phase with every other; this phase difference must therefore correspond to a real distance (path difference) which equals an integral multiple of the wavelength.

This happens, for example, when the path difference is one wavelength, in which case we speak of the positive first diffraction order (m = 1) or the negative first diffraction order (m= −1), depending on whether the rays are advanced or retarded as we move from groove to groove. Similarly, the second order (m = 2) and negative second order (m = −2) are those for which the path difference between rays diffracted from adjacent grooves equals two wavelengths.

The grating equation reveals that only those spectral orders for which $|\, m\lambda/d| < 2$ can exist; otherwise, $|\sin\alpha + \sin\beta| > 2$, which is physically meaningless. This restriction prevents light of wavelength λ from being diffracted in more than a finite number of orders.

Specular reflection *(*m = 0*)* is always possible; that is, the zero order always exists (it simply requires $\beta = -\alpha$). In most cases, the grating equation allows light of wavelength λ to be diffracted into both negative and positive orders as well. Explicitly, spectra of all

orders m exist for which $-2d < m\lambda < 2d$, m an integer. For $\lambda/d << 1$, a large number of diffracted orders will exist. As seen from Equation (4.1), the distinction between negative and positive spectral orders is that

$\beta > -\alpha$ for positive orders (m > 0),

$\beta < -\alpha$ for negative orders (m < 0).

$\beta = -\alpha$ for specular reflection (m = 0).

This sign convention for m requires that m > 0 if the diffracted ray lies to the left (the counter-clockwise side) of the zero order (m = 0), and m < 0 if the diffracted ray lies to the right (the clockwise side) of the zero order. This convention is shown graphically in Figure (4.3).[8]

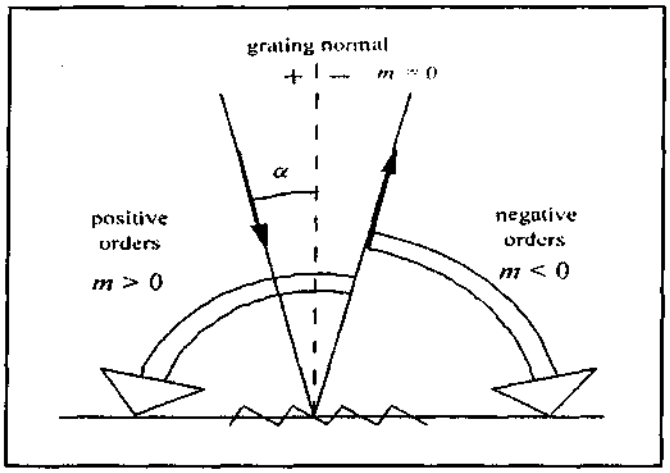

Figure (4.3): Sign convention for the spectral order m.

(4.3) Dispersion :

Dispersion is a measure of the separation (either angular or spatial) between diffracted light of different wavelengths. Angular dispersion expresses the spectral range per unit angle, and linear resolution expresses the spectral range per unit length.

Angular Dispersion

The angular spread $\Delta\beta$ of a spectrum of order m between the wavelength λ and $\lambda + \Delta\lambda$ can be obtained by differentiating the grating equation, assuming the incidence angle α to be constant. The change D in diffraction angle per unit wavelength is therefore

$$D = \frac{d\beta}{d\lambda} = \frac{m}{d\cos\beta} = \frac{m}{d}\sec\beta = Gm\sec\beta \tag{4.3}$$

The quantity D is called the angular dispersion. As the groove frequency G = 1/d (d groove spacing) increases, the angular dispersion increases (meaning that the angular separation between wavelengths increases for a given order m).

Linear Dispersion

For a given diffracted wavelength λ in order m (which corresponds to an angle of diffraction β), the linear dispersion of a grating system is the product of the angular dispersion D and the effective focal length r'(β) of the system:

$$r'D = r'\frac{d\beta}{d\lambda} = \frac{mr'}{d\cos\beta} = \frac{mr'}{d}\sec\beta = Gmr'\sec\beta \tag{4.4}$$

We have written r'(β) for the focal length to show explicitly that it may depend on the diffraction angle β (which, in turn, depends on λ). The reciprocal linear dispersion, sometimes called the plate factor P, is more often considered; it is simply the reciprocal of r' D, usually measured in nm/mm:

$$P = \frac{d\cos\beta}{mr'} \tag{4.5}$$

P is a measure of the change in wavelength corresponding to a change in location along the spectrum (in mm).[8]

(4.4) Resolving Power :

Resolving power R of a grating is a measure of its ability to separate adjacent spectral lines of average wavelength λ. It is usually expressed as the dimensionless quantity

$$R = \frac{\lambda}{\Delta\lambda} \tag{4.6}$$

Here $\Delta\lambda$ is the limit of resolution, the difference in wavelength between two lines of equal intensity that can be distinguished (that is the peaks of two wavelengths λ_1 and λ_2 for which the separation $|\lambda_1 - \lambda_2| < \Delta\lambda$ will be ambiguous).[8]

Chapter-5

Vacuum Ultraviolet Spectrographs and Their Working

Spectrographs are available in many different types and the selection of an all purpose instrument allows a certain degree of choice. In making such a choice things to be considered are, the range of wavelengths over which the spectrograph can be used, the extent to which it disperses light, the variation of this dispersion with wavelength, the resolving power of the instrument, and the brightness of the spectrum that it produces. Other important but secondary considerations are freedom from scattered light, suitable shape and size of the spectral lines produced and ease of adjustment.

There are two basic types of spectrographs for the vacuum ultraviolet region.
(a) Normal incidence mount which is suitable to study the wavelengths from 300 Å to 2000 Å.
(b) Grazing incidence mount which is suitable to study the wavelengths below 300 Å.

At the Physics Department of Aligarh Muslim University, various types of spectrographs are available for recording in air including 1.5-metre, 21-feet, and 35-feet grating spectrographs. A 3-metre normal incidence grating spectrograph is also available for vacuum ultraviolet region.

(5.1) Normal Incidence Spectrograph :

When the angle of incidence α is less than approximately 10°, the radiation is considered to be directed at normal incidence to the grating. For α less than 10°, there is very little astigmatism and essentially no change in the reflectance, hence efficiency, of the grating. Figure (5.1) shows the optical layout of the spectrograph and figure (5.2) shows the normal incidence spectrograph.[7]

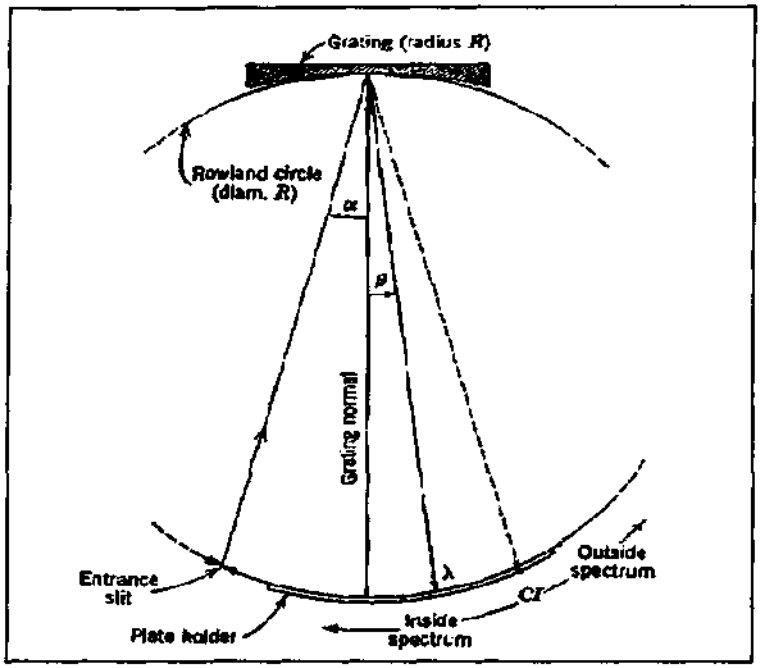

Figure (5.1): Optical layout of a basic spectrograph

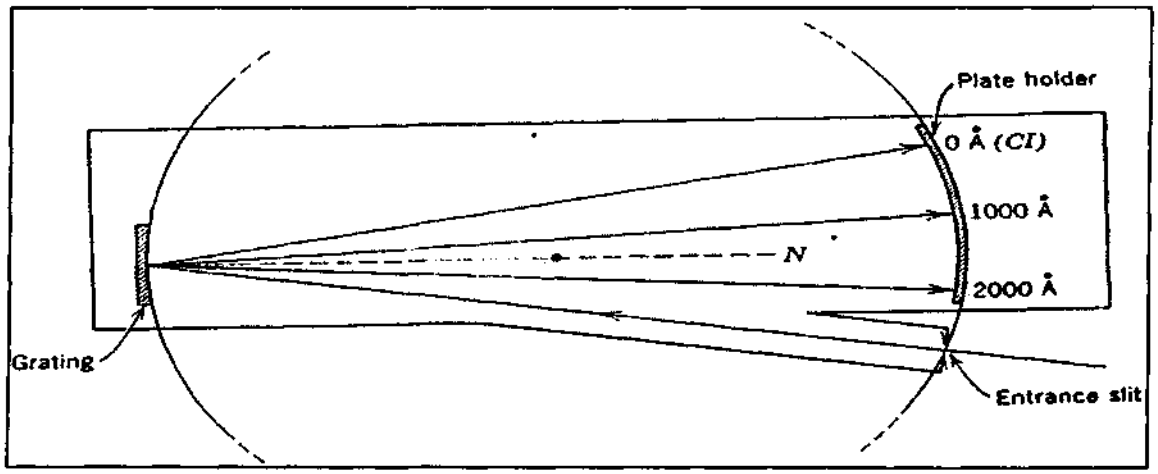

Figure (5.2): Normal incidence spectrograph

(5.2) Grazing Incidence Spectrograph :

When the angle of incidence α is approximately 89^0, the radiation is considered to be directed at grazing incidence to the grating. By this spectrograph the shortest wavelengths can be photographed lie at about 200 Å. With increase in the angle of incidence, the astigmatism of the grating increases rapidly. Figure (5.3) shows the grazing incidence spectrograph.[7]

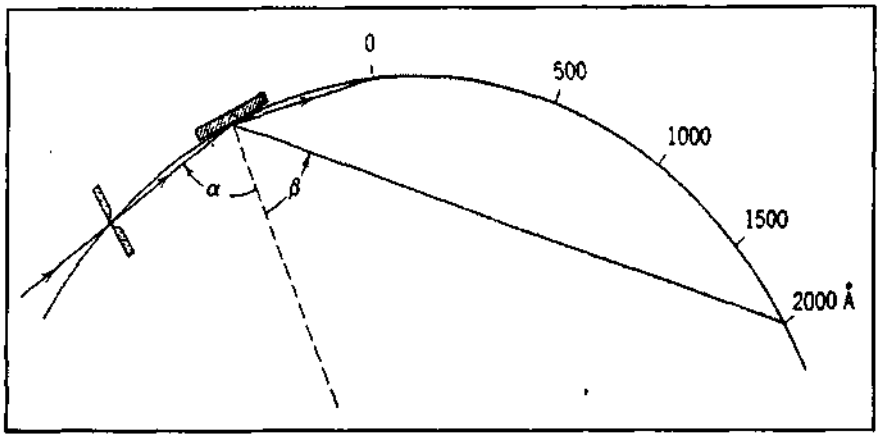

Figure (5.3): Grazing incidence spectrograph

(5.3) Different Types Of Mounting :

In selecting a mounting, we should consider the grating orders to be used, the wavelengths range to be covered, the degree of astigmatism that can be tolerated, the brightness of the resulting spectra, the freedom from spurious lines (which may depend on angle), and the departure from uniform dispersion (smallest on the normal).

The six mountings of concave gratings most commonly used are

a) The Rowland Mounting
b) The Eagle Mounting
c) The Paschen-Runge Mounting
d) The Abney Mounting
e) The Wadsworth Stigmatic Mounting
f) The Radius Mounting

Eagle mounting is used in our 3-metre vacuum spectrograph. Here we will describe Rowland and Eagle mountings. Eagle mounting is based on the principle of Rowland mounting. In common with the Rowland mounting, Eagle mounting uses the angle-in-a-semicircle theorem.

(1) The Rowland Mounting :

The oldest concave grating mounting invented and constructed by Rowland and described in 1883, that the slit, grating, and the plate holder shall lie on the Rowland circle. The grating and the plate holder are fastened on the opposite ends of a long, rigid

bar so that the distance between the grating center and the middle point of the plate holder is equal to the radius of curvature (R) of the blank, while the plate holder has the curvature of the Rowland circle with a radius R/2. It can easily be observed that the center of the grating, the slit and the plate is located on an exact circle, since, the right angle whose sides go through the grating and the plate holder center is always inscribed in the circle whose radius is the diameter of the Rowland circle.[6]

The disadvantage of the Rowland mounting are that only a limited region of the spectrum can be photographed at one setting; that it has a high degree of astigmatism, so that much intensity may be lost, especially in the higher orders; and that the highest orders of the grating cannot be reached. In this mounting the grating and plate holder both move is a disadvantage.[9]

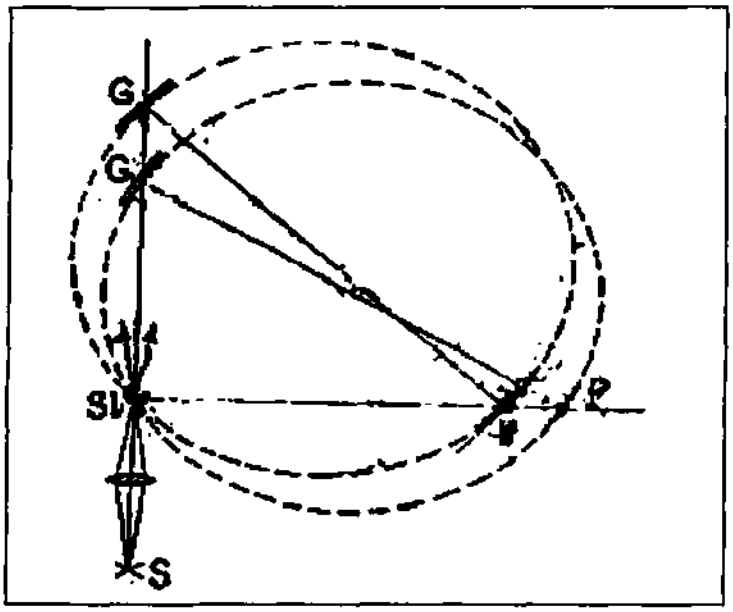

Figure (5.4): The Rowland mounting of the concave grating

(2) <u>The Eagle Mounting :</u>

This mounting is used in our vacuum spectrograph. It keeps astigmatism as low as is possible. This mounting occupies a long narrow space. Higher orders can be reached than in the Rowland Mounting and the astigmatism is less.

The Eagle Mounting of the concave grating is similar to the Littrow mounting of the plane grating, but it is superior because no lens is needed, so that it can be used in all

spectral regions. In this mounting slit and plate holder are mounted close together on one end of a rigid bar, on the other end a concave grating is mounted.[9]

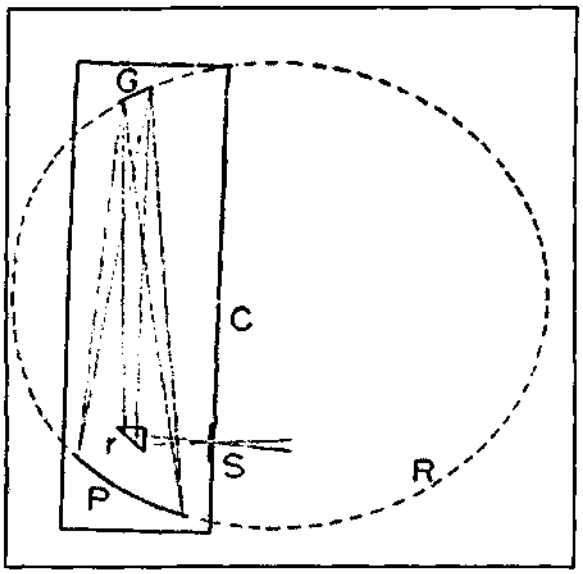

Figure (5.5): Eagle mounting of the concave grating. R, Rowland circle; S, Slit; r, Reflecting prism; G, Concave grating; P, Plate; C, Light tight case

(5.4) Vacuum Spectrograph With Three Metre Grating :

A range of vacuum grating spectrographs are available for emission and absorption spectroscopy at wavelengths shorter than the transmission limit of the atmosphere. For work down to about 400 Å a reflection grating, positioned at approximately normal incidence, may be used, and instruments can be provided with 1, 2, or 3-metre radius concave gratings, according to the dispersion required.

For shorter wavelengths it is necessary to use a grating at a sufficiently large angle of incidence for total reflection to occur, and 2 and 3 m radius grazing incidence concave grating spectrographs are made for this purpose. The basic arrangement of the instruments follows conventional lines, but the designs have been made in accordance with modern high vacuum technique, which allows rapid pumping and easily demounted and reliable vacuum seals. Attention has been paid to distortion which could occur on evacuation.[10]

A grating used at approximately normal incidence confers many advantages on a spectrograph if wavelength below about 400 Å is not to be recorded. Its astigmatism is much less than that of a grating at grazing incidence, its effective aperture is greater, and

on both accounts it allows far shorter exposures. Hilger built a normal incidence vacuum spectrograph based on a design by Sawyer. A normal incidence grating, with 3-metre radius of curvature, is used in this vacuum spectrograph, shown below.[11]

Figure (5.6): Vacuum spectrograph with 3-metre grating at normal incidence

Grating characteristics of 3-metre vacuum spectrograph at department of physics, A.M.U., Aligarh

Bausch and Lomb corporate, Rochester New York, USA

Certified Precision Grating Catalogue No.	3552-53-710
Serial No.	2482-4-4
Grooves/mm	1200
Blaze angle	$5^0\ 10'$
Concave radius	2998.3 mm
Grating area	$52 \times 80\ mm^2$

Figure (5.7): Vacuum spectrograph with 3-metre grating at normal incidence installed at Spectroscopy Lab of Physics Department A.M.U. Aligarh

In the 3-m normal incidence vacuum grating spectrograph, type E865, a fixed slit is provided and is sealed with O-rings. The slit mount terminates in a flat surface to which any source may be sealed by a ring seal. Behind the slit is a flap valve which may be used to seal the spectrograph from the source when changing source conditions. The grating is lightly ruled on aluminized glass to give high energy in the vacuum ultra-violet and has a ruled area of $4\frac{1}{2} \times 8$ cm. The spacing is 14400 lines per inch. It is mounted in such a way as to allow its rotation about three mutually perpendicular axes and its longitudinal movement for focusing.

The plate holder, which can be adjusted to the correct tilt, takes $6\frac{1}{2} \times 1\frac{1}{2}$ in. plates. The plate can be racked up or down by means of an external control, and it is arranged so that the shutter of the dark slide automatically shuts at the end of the plate motion. The plate length allows a spectral range about 1250 Å in the first order. The camera housing can be sealed from the main spectrograph by an external control, allowing the plate to be

changed without breaking the main vacuum. Separate diffusion and rotary pumps can be provided on the camera if required.[10]
The dispersion is almost constant (about 6 Å/mm in the first order) throughout the spectrum, and adjustments are not critical. The instrument has been designed with a view to future supplementation by photoelectric recording.

All controls are external and are provided with dials giving a clear indication of their setting. There is a control for racking the plate so that successive spectra up to 6 mm wide can be photographed without opening the instrument, another for adjusting a metal screen that has the effect of a Hartmann diaphragm with three aperture 2 mm high, another for adjusting the width of the slit to a maximum of 2 mm, and a fourth for selecting the wavelength range.

The shortest wavelength that the spectrograph can record is about 400 Å and the longest about 2900 Å. The plate size is 10 ×2 in. The light source can be sealed to the spectrograph by means of an O-ring seal. Gas leakage from the source is reduced as far as possible by a secondary, fixed, slit little more than 2 mm wide, but for work on the longer wavelengths a fluoride window can be fitted to provide a perfect seal. If components such as absorption cells with fluoride windows are to be used, they can be supported on the 21 in. accessory bar for which the instrument makes provision. The instrument stands on two cabinets, one serving as a cupboard and the other housing the pumping equipment.[11]

The vacuum pressures are measured by a two-head, two-range, Pirani gauge, Edwards type 7-2A. One head is connected in the backing line and the other to the spectrograph. The two pressure ranges covered are 1.0 to 0.005 and 0.005 to 0.0001 mm of Hg. If the separate pumping system for the camera is used, a model 6-2 Pirani gauge is provided with four gauge heads to allow each backing and high vacuum pressure to be measured. This instrument can accommodate a further two gauge heads, which may be convenient for measuring source pressures.[10]

Chapter-6

Vacuum Techniques

(With reference to our 3-m vacuum ultraviolet spectrograph)

Latin word VACUUS means "empty". Why is a vacuum needed?

(1) To move a particle in a (straight) line over a large distance.

(2) To provide a clean surface. Basically atmosphere is contaminant (usually water).

(3) To prevent attenuation of the radiation from the light source depends on the wavelength and the pathlength from the entrance slit to the plateholder via the diffraction grating.

(6.1) Vacuum Pumps :

Vacuum pumps can be divided into the following categories:

i. Positive displacement type
ii. Momentum transfer type
iii. Cryo pumps
iv. Sorption pumps
v. Ion pumps

Positive displacement pumps are the most effective for low vacuums. Momentum transfer pumps associated with one or two positive displacement pumps are the most common configuration used to achieve high vacuum. In this configuration the positive displacement pump serves two purposes.

First it obtains a rough vacuum in the vessel being evacuated (before the momentum transfer pump can be used to obtain the high vacuum), as momentum transfer pumps cannot start pumping at atmospheric pressures.

Second the positive displacement pump backs up the momentum transfer pump by evacuating to low vacuum the accumulation of displaced molecules in the high vacuum pump. Rotary pump and Diffusion pump were associated to our vacuum spectrograph.

(6.2) Oil-Sealed Rotary-Vane Pump :

The oil-sealed rotary vane pump, also known as the rotary pump, belongs to the positive displacement class. It is low vacuum and roughing pump. We can achieve the vacuum of the order of 10^{-3} Torr by this pump.

The rotary pump is constituted of a stator and an eccentrically positioned rotor. The stator or the casing is a steel cylinder, the ends of which are closed by suitable plates which hold the shaft of the rotor. The stator is pierced by the inlet and the exhaust ports which are positioned respectively a few degrees on either side of the vertical. The inlet port is connected to the vacuum system. The exhaust port is provided with an outlet valve.

The rotor consists of a steel cylinder, mounted on a driving shaft. Its axis is parallel to the axis of the stator but is displaced from the axis (hence eccentric), such that it makes contact with the top surface of the stator, the line of contact lying between the two ports. This line of contact is known as the top seal between stator and rotor. A diametrical slot is cut through the length of the rotor and carries the two vanes. The vanes are rectangular steel plates which make a sliding fit in the rotor slot and are held apart by a spring. This ensures that the rounded edge of the vanes always make good contact with the stator wall. The whole of the stator rotor assembly is submerged in suitable oil.

The rotary pump oil should posses some desirable characteristics. These are high viscosity, low vapour pressure and high temperature resistance. It is usually low vapour pressure hydrocarbon oil (Polyphenyl ether or Alkyl-naphthalene).

The working consists of three stages: Suction, Compression and Exhaust. As the vane A passes the inlet port (figure 6.1a), the vacuum system is connected to the space limited by the stator, the top seal, the rotor and vane A. The volume of this space increases as the vanes sweep round and produces a pressure decrease in the system. This continues until vane B reaches the inlet port (figure 6.1b), when the volume of the gas evacuated is isolated between the two vanes. Further rotation sweeps the isolated gas around the stator until vane A passes the top seal (figure 6.1c). The gas is now held between vane B and

the top seal and by further rotation it is compressed until the pressure is sufficient (about 850 Torr) to open the exhaust valve and the gas is evacuated from the pump.[12]

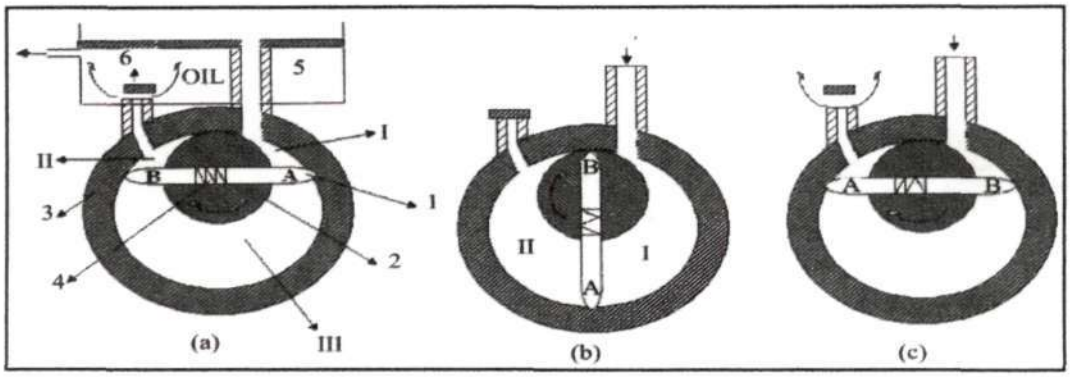

Figure (6.1): Three Stages of Rotary Oil Pump

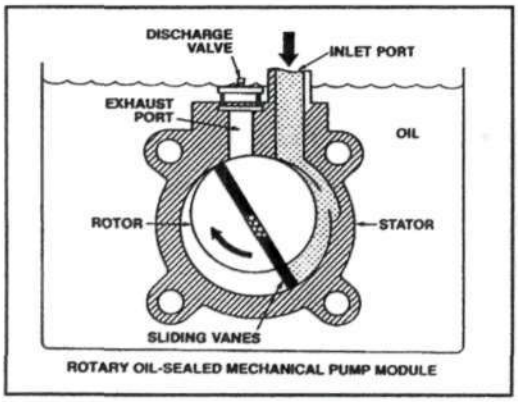

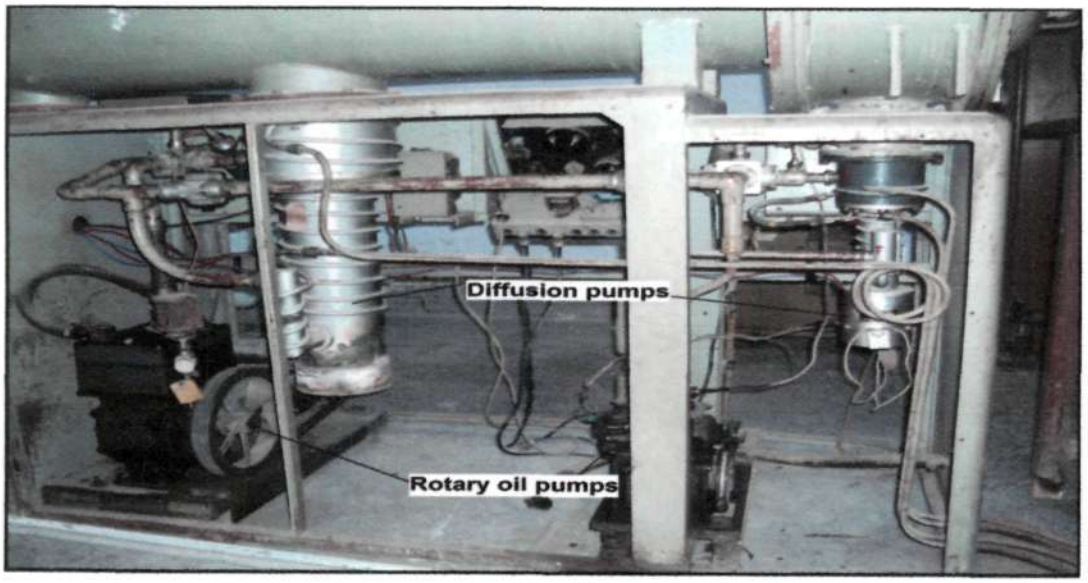

Figure (6.2): Rotary pump and Diffusion pump associated with spectrograph

The advantages of a rotary oil pump are the following:

(1) It is driven by an electric motor and the whole operation is quick and automatic, with no man power needed.

(2) Due to a much higher speed of rotation of the rotor, it can produce a much higher degree of vacuum.

(3) Its being kept immersed in oil automatically ensures its efficient cooling and lubrication as also prevents leakage of the gas or vapor into the vacuum produced.

(4) It can operate directly from the atmospheric pressure and no fore-vacuum is necessary.

(5) It is small and compact in size and occupies much less space.

(6.3) Diffusion Pump :

This high vacuum pump operates in the range from 10^{-3} Torr to 10^{-7} Torr. We achieved the vacuum of the order of 10^{-5} Torr by this pump. It can not operate directly from the atmospheric pressure but requires a fore-vacuum ranging from 20 mm to 10^{-3} mm. The principle is that in a mixture of gases, the diffusion of a gas takes place from a region where its partial pressure is higher to that where it is lower, irrespective of the total pressure in the two regions.

The development of the diffusion pump was made by Gaede in 1913 using mercury as the pump fluid. A diffusion pump consists of a cylindrical body fitted with a flanged inlet for attachment to the system to be evacuated. The bottom of the cylinder is closed forming the boiler which is fitted with a heater. The upper two thirds of the body is surrounded by cooling coils. An outlet duct or foreline is provided at the side of the lower pump body for discharging the pumped gases and vapours to the mechanical fore pump. A suitable oil called pump fluid or working fluid is taken at the bottom of the boiler. These are phenyl siloxane compounds.

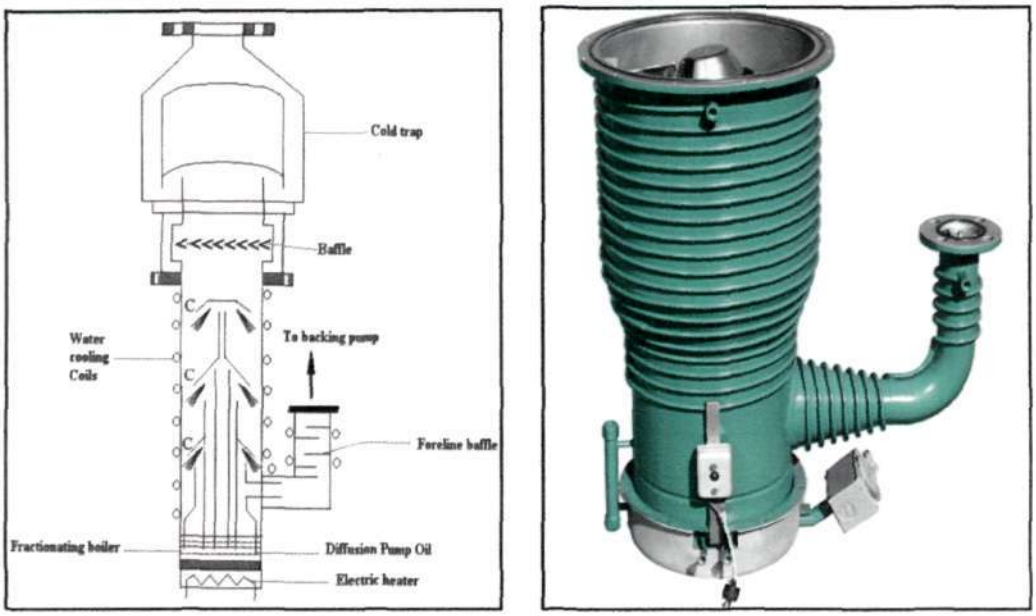

Figure (6.3): Diffusion Pump

A jet forming structure can be seen within the pump body. This consists of a concentric cylinder partially capped and fitted with flared ends to form umbrella shaped jets through which the pump fluid vapours can emerge at supersonic speeds (shown by arrows). This portion is called Chimney (designated by C). There are no moving mechanical parts in *diffusion pumps*.

The chamber to be evacuated and the diffusion pump are separated by the Baffle Valve. The chamber and the diffusion pump can be independently roughed by closing the appropriate valve to the fore pump. After the initial pumping of both sides to nearly 10^{-1} Torr, the valve connecting the chamber to the fore pump is closed and simultaneously the baffle valve is opened. Now the diffusion pump is ready for operation.

During the operation the working fluid in the boiler of the pump is heated by means of an electric heating coil clamped to the lower body and a vapour stream is created. This vapour rises in the jet forming structure and is emitted at supersonic speeds through the annular nozzle in a downward and outward direction against the water-cooled wall of the pump body.

Gas molecules arriving at the pump inlet are entrained in the stream of the working fluid vapour and are given a downward momentum. The gas-vapour mixture travels downward towards the foreline. When the oil vapour constituents of such a jet stream strikes the water cooled wall of the pump body, they are condensed and returned to the boiler in the liquid form. The entrained gas molecules continue their flow towards the exit where they are removed by the mechanical forepump. The condensed oil vapours returned to the boiler get re-evaporated and maintains the vapour flow to the jet assembly.[12]

(6.4) Vacuum Gauges :

Vacuum gauges are of two types one is Direct Reading Type and other is Indirect Reading Type. In the direct reading type of vacuum gauges, transducers that measure the pressure by means of the force exerted by the gas on a suitable surface are used. In the second type of gauges, the pressure is determined by a property of the gas which depends on the pressure.

Direct Reading Vacuum Gauges:

- Liquid Column Manometer
- McLeod Gauge

Indirect Reading Vacuum Gauges:

- Pirani Gauge
- Thermocouple Gauge
- Ionization Gauges

(6.5) Pirani Gauge :

Here we used the Pirani Gauge to measure pressure inside the vacuum chamber. It is a well known fact that whereas at high and ordinary pressures, the thermal conductivity of a gas (K) is quite independent of pressure, at pressures below 10^{-3} mm, it is directly proportional to pressure, i.e., K is linear function of p. This fact was first used by Warburg, in 1907, for the measurement of low pressures and forms the basis of the Pirani gauge. In construction, it is very much like the cage-type incandescent lamp.

The essential requirements are:

(i) The filament should have a high coefficient of increase of resistance with temperature, so that even a small change in its temperature may result in an appreciable change in its resistance,

(ii) The heat-loss along the filament support should be as small as possible,

(iii) The distance between the filament and the wall of enclosing glass bulb must remain unaltered.

With change in pressure of the gas between the filament and the wall of the bulb, the rate of conduction of heat across the gas changes. This results in a change in the temperature of the filament and hence a change in its resistance. The change in the resistance of the filament is measured by a Wheatstone's bridge. It gives the change in conductivity of the gas and hence, indirectly through a calibration curve, the pressure of the gas (measured by Mcleod Gauge).[13]

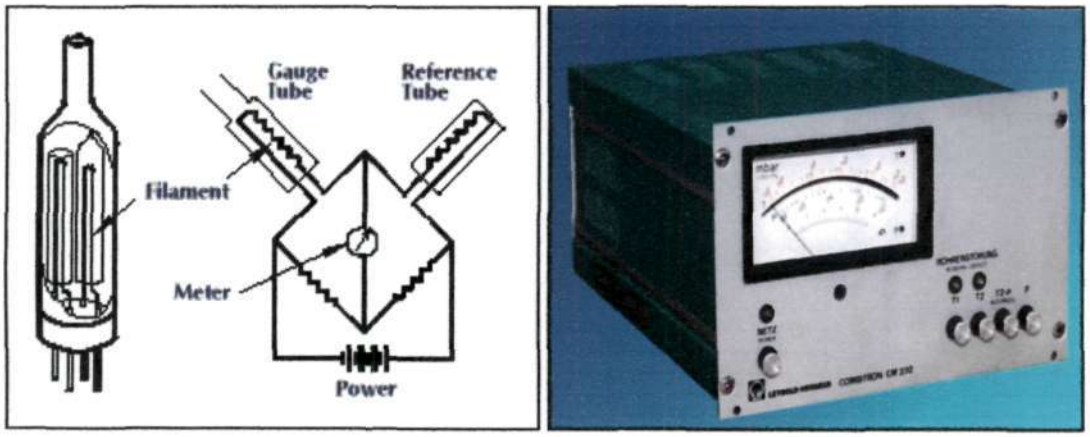

Figure (6.4): Pirani Gauge

Chapter -7

Recording of Spectrum and Measurement of Wavelengths

The spark source designed by us in our department is fitted with the 3-metre vacuum spectrograph as shown in figure (3.2).The other feature of this design is discussed in section (3.3). In this spark source, two electrodes of any material can be mounted at a fixed gap of 5 mm or so.

(7.1) Calibration of Spectrograph :

The calibration of spectrograph is achieved, by calibrating different spectral region. A wheel at the center of long cylinder of spectrograph is used to select different spectral region by moving the grating attached to it. The wheel is rotated either clockwise or anticlockwise, to select different spectral regions. A copper arc is placed infront of the slit, outside the spectrograph. The arc is aligned with grating for maximum intensity of light at the middle of the grating. Initially the slit width of the spectrograph was kept open wide so that the persistent lines and their intensities could be recorded for different exposer times. On recorded spectrum, the resonance lines of copper 3247.550 Å and 3273.967 Å can easily be identified as shown in figure (7.1). These lines are brought to one end of the plate so that the lower wavelengths could also be recorded. The spectral region wheel is rotated to record a spectrum which contains few known lines of previously recorded spectrum at one end, the wheel is marked for these lines to select spectral region. The figures from (7.1) to (7.3) show copper arc spectrum. After marking different spectral regions with the wheel, the slit width is optimized to record the copper arc spectrum on X-ray film figure (7.4).

Figure (7.1): Copper arc spectrum in air

Figure (7.2): Copper arc spectrum in air

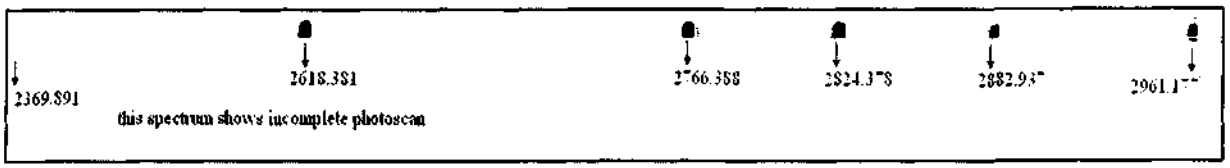

Figure (7.3): Copper arc spectrum in air

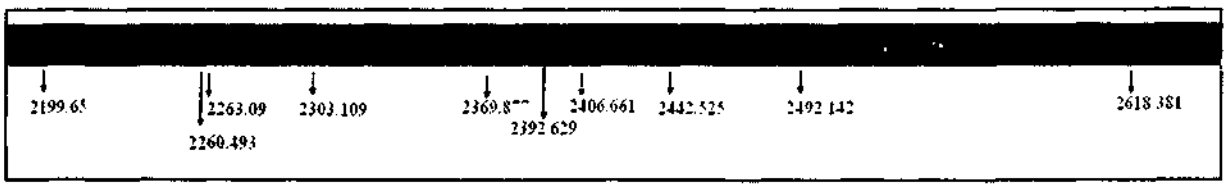

Figure (7.4): Copper arc spectrum in air on x-ray film

(7.2) Mounting and Alignment of Spark chamber :

To mount the spark chamber for the first time, the spark chamber's side covers were removed and copper electrodes are fixed at their post in the spark chamber [Figure 7.5]. The rear side cover {as shown in Figure (3.2)} of the spectrograph is removed. The copper electrodes are connected to spark power supply at the possible lower voltage and with low capacity condenser. The center of spark was observed near grating on a paper, keeping the slit of spectrograph open wide. If the spark spot on the paper do not lie at the middle of the grating, the spark gap between the electrodes may be shifted to either side to get maximum brightness at middle of the grating. The center of the spark gap was measured diametrically with respect to the circumference of the electrode holder plate with a fixed mark on it. Now it is possible to adjust these electrodes for required spark gap between them. It is the center of these electrodes which is aligned with the grating. We cover the rear side of the spectrograph and reduce the slit width to the desired limit for recoding the spectrum as shown in Figure (7.6).

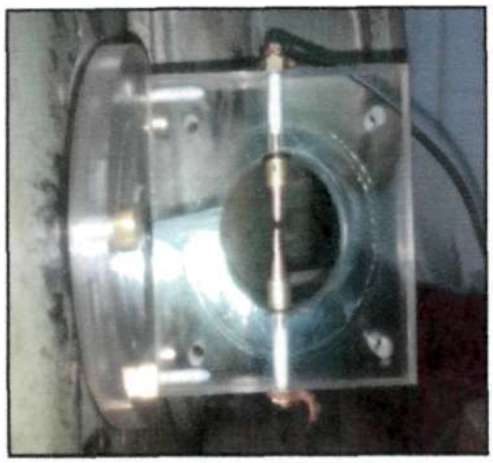

Figure (7.5): Spark Chamber without side cover

Figure (7.6): Spark Chamber with side cover

(7.3) Recording of Zinc spectrum :

The spectrograph is calibrated for spectral region and aligned with Spark chamber as discussed in section (7.1) and (7.2). The Zinc spectrum is recorded on X-ray film. The X-ray film "FUJI MEDICAL X-RAY FILM" Super RX, blue sensitive was used. The commercially available Zinc and copper electrodes were used to record spectrum which might have some impurities also. Some zinc spark lines in this region are found hazy as also reported by R. O. Hutchinson [14], is shown below in figure (7.8). For calibration of lines, a copper spark spectrum (half height) and Zinc spectrum (full height) is recorded on the same film as shown in figure (7.7). The intensity of observed lines is the visual estimate of blackening of the film.

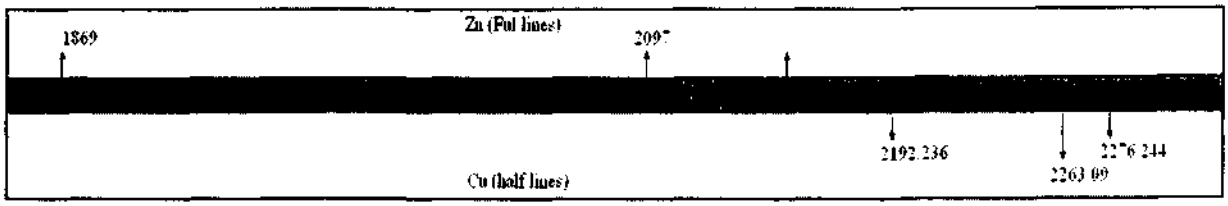

Figure (7.7): Copper and Zinc spark spectrum in vacuum

Figure (7.8): Zinc spark spectrum in vacuum

(7.4) Development and Fixing :

The X-ray film after recording the spectrum was developed for six minutes in the dark room of our spectroscopy lab with the ordinary developer used for photographic films. The film was washed and put into hypo solution for four minutes, then again washed properly with fresh water.

(7.5) Measurement of Wavelengths :

The positions of Copper as well as Zinc lines are measured simultaneously on Carl Zeiss Abbe comparator. The previously known copper lines are used as internal standards for calculation of wavelengths. The wavelengths of lines for their corresponding positions are calculated by using a programme called MOSFIT. The Mosfit programme was developed by G.J. VAN HET HOF for polynomial fit of some impurities lines, these known lines are called internal standards [15]. The Zinc observed lines are given in table (7.1). The inductance can be purposefully introduced in series with the light source to help identify the state of ionization producing unknown lines. The radiation from the most highly ionized atoms disappears first as the series inductance is increased [7]. The ionization separation was done by recording different spectrums on the same plate by varying the series inductance in figure (5.7). The line list of Zn I, II and III are available at the website hosted by the Department of Physics and Astronomy, University of Kentucky.[16]

Table (7.1) Observed lines of Zinc :

Observed Wavelengths (Å)	Ions Affiliation
1869.9473	Zn III
1942.9709	Zn III
1979.5234	Zn III
1982.1207	Zn III
2033.9146	Zn III
2036.3978	Zn III
2054.6521	Zn III
2062.4983	Zn II
2087.3915	Zn III
2097.7905	Zn III
2110.2740	Zn III
2121.4536	Zn III
2139.7958	Zn I
2142.2512	Zn III
2153.2796	Zn III
2159.2594	Zn II
2163.4539	Zn III
2193.9641	Zn III
2216.6543	Zn III
2246.0916	Zn III
2249.0291	Zn III
2252.5723	Zn III
2256.0540	Zn III
2266.3090	Zn III
2271.2040	Zn III
2274.7701	Zn III
2282.4148	Zn III

2286.3870	Zn III
2290.2114	Zn III
2321.8482	Zn III
2327.9247	Zn I
2329.1946	Zn I
2333.9546	Zn III
2346.0833	Zn III
2347.0059	Zn III
2347.7799	Zn I

Chapter-8

Results and Discussion

(8.1) Zn I and Zn II spectra :

We have identified some lines of Zn I and Zn II but there is majority of Zn III lines on our spectrogram. So some informations of Zn I and Zn II are given here. The ground state configuration of Zn I is $1s^2 2s^2 2p^6 3s^2 3p^6 3d^{10} 4s^2$ which has 30 electrons with $^1S_0$ as the ground level. The excited state configurations are 4s4p, 4s5p, 4s6p, 4s5s, 4s6s, 4s7s, and 4s4d etc. Some configuration and their levels are listed below:

Configuration	Term	J
$4s^2$	^1S	0
4s4p	$^3P^0$	0, 1, 2
	$^1P^0$	1
4s5s	^3S	1
	^1S	0

The four Zn I transition observed are the following:

Transitions	Corresponding wavelengths
$4s^2$ - 4s4p	2139.7958 Å
4s4p - 4s.20d	2327.9247 Å
4s4p - 4s19d	2329.1946 Å
4s4p - 4s14d	2347.7799 Å

The ground state configuration of Zn II is $1s^2 2s^2 2p^6 3s^2 3p^6 3d^{10} 4s$ which has 29 electrons with $^2S_{1/2}$ as the ground level. The excited configurations are $3d^{10}4p$, $3d^{10}5p$, $3d^{10}5s$, $3d^{10}6s$, $3d^{10}4d$ etc. A few excited configurations with their levels are listed below:

Configuration	Term	J
$3d^{10}4p$	$^2P^0$	1/2, 3/2
$3d^{10}5s$	^2S	1/2
$3d^{10}4d$	^2D	3/2, 5/2

Only two observed Zn II transition are the following:

Transitions	Corresponding wavelengths
$3d^{10}4s - 3d^{10}4p$	2062.4983 Å
$3d^{9}4s^{2} - 3d^{9}4s4p$	2159.2594 Å

(8.2) Spectral Analysis of Zinc III :

The Zinc spectrum below 2000 Å was recorded on vacuum grating spectrograph by R. A. Sawyer [17]. R. O. Hutchinson too recorded the zinc spectrum below 2146 Å up to 465.5 Å. He also mentioned in his table, and characterized the zinc lines as broad hazy [14]. The wavelength material available in the paper of Sawyer was not reliable [18]. Laporte and Lang reported the first observation of Zn III spectrum with vacuum spark which could be used to classify 38 measured lines [19]. The line list given in the paper is spread our observed region. The copper and zinc spectra were recorded on the same plate with different height. The known copper lines were taken as standards to find zinc lines. The ground state configuration of Zinc III is $1s^{2}2s^{2}2p^{6}3s^{2}3p^{6}3d^{10}$ which has 28 electrons with $^{1}S_{0}$ as the ground level. Some of the excited state configurations are $3d^{9}4s$, $3d^{9}4d$, $3d^{9}5g$, $3d^{8}4s^{2}$, $3d^{9}4p$, $3d^{9}4f$ and $3d^{8}4s4p$. A few excited configurations and the number of their energy levels are given below.

$3d^{9}4s$: 04
$3d^{9}4d$: 18
$3d^{9}5g$: 20
$3d^{8}4s^{2}$: 08
$3d^{9}4p$: 12
$3d^{9}4f$: 20
$3d^{8}4s4p$: 89

The spectrum was recorded in the region (1850-2350 Å). These wavelengths were assigned their respective ionic species which were further verified according to wavelengths table available at website [16]. Some oxygen lines were also observed but not included in the observed wavelength table. We observed 11 and 2 transitions of even parity configurations $3d^{9}4d$ and $3d^{8}4s^{2}$ respectively and 9, 2, 1 and 1 transitions from odd

parity configurations $3d^8 4s4p$, $3d^9 4f$, $3d^9 5p$ and $3d^9 6p$ respectively. The Observed wavelengths and their corresponding transitions are given in table (V).

(8.3) Theoretical Interpretation of Zinc III Spectrum :

The R.D. Cowan's Computer code [5] has been used to predict the energy level structure and associated transition probabilities. In the even parity system $3d^{10}$, $3d^9 4s$, $3d^9 5s$, $3d^9 6s$, $3d^9 7s$, $3d^9 8s$, $3d^9 9s$, $3d^9 4d$, $3d^9 5d$, $3d^9 6d$, $3d^9 5g$, $3d^9 6g$, $3d^9 7g$, $3d^9 8g$ and $3d^8 4s^2$ configurations were considered for configuration interaction effect while $3d^9 4p$, $3d^9 5p$, $3d^9 6p$, $3d^9 4f$, $3d^9 5f$ and $3d^8 4s4p$ were mixed for odd parity configurations.

The ab initio scaling of the energy parameters were as:

E_{av} and ζ = 100 % of HFR values.

F^k = 85 % of HFR values.

G^k = 75 % of HFR values.

R^k = 80 % of HFR values.

After having reliable predictions, analysis was carried out in the guidance of predicted transition probabilities. The levels were used to run least squares fitted (LSF) parametric calculations. This allowed adjusting the energy parameters to the real values and hence a better prediction was achieved. The major contribution of this least squares calculations is that the large numbers of unknown levels are now predicted with much better accuracy. All the observed and least squares fitted energy levels of even and odd parity configurations are given in table I and table II respectively along with their LS percentage compositions. All the least squares fitted energy parameters of even and odd parity configurations are given in table III and IV respectively.

The configuration gross structure with possible transitions between them has been shown in Grotorian diagram [figure (8.1)].

Table I.

Observed and least squares fitted energy levels of even parity configuration of Zn III in Cm^{-1} :

J	E(obs)	E(LSF)	diff.	LS-composition.
1				
0	0.0	0.0	0.0	99% 3d10
	212340.3	212657.0	-316.7	92% 3d8 4s2 <2>3P + 8% 3d9 4d 3P
	218428.0	218737.0	-309.0	91% 3d9 4d 3P + 8% 3d8 4s2 <2>3P
	-	231466.0	-	81% 3d9 4d 1S + 16% 3d9 5d 1S
	-	252361.0	-	98% 3d9 5d 3P
	-	256544.0	-	98% 3d8 4s2 <0>1S
	-	261818.0	-	64% 3d9 5d 1S + 26% 3d9 6d 1S + 7% 3d9 4d 1S
	-	273198.0	-	99% 3d9 6d 3P
	-	284156.0	-	72% 3d9 6d 1S + 17% 3d9 5d 1S + 10% 3d9 4d 1S
1	80850.2	81076.0	-225.8	100% 3d9 4s 3D
	211920.7	212240.0	-319.3	90% 3d8 4s2 <2>3P + 8% 3d9 4d 3P
	214357.0	215133.0	-776.0	87% 3d9 4d 3S + 5% 3d9 4d 3P + 5% 3d9 4d 1P
	216895.4	217027.0	-131.6	53% 3d9 4d 1P + 22% 3d9 4d 3D + 17% 3d9 4d 3P + 4% 3d9 5s 3D
	217663.7	217680.0	-16.3	94% 3d9 5s 3D + 4% 3d9 4d 1P
	218909.3	219173.0	-263.7	54% 3d9 4d 3P + 28% 3d9 4d 1P + 12% 3d9 4d 3S
	220006.6	220030.0	-23.4	75% 3d9 4d 3D + 14% 3d9 4d 3P + 9% 3d9 4d 1P
	-	250255.0	-	73% 3d9 5d 3S + 19% 3d9 5d 3P + 8% 3d9 5d 1P
	-	250898.0	-	50% 3d9 5d 1P + 26% 3d9 5d 3D + 23% 3d9 5d 3P
	-	252836.0	-	98% 3d9 6s 3D
	-	253293.0	-	47% 3d9 5d 3P + 27% 3d9 5d 3S + 26% 3d9 5d 1P
	-	253748.0	-	72% 3d9 5d 3D + 15% 3d9 5d 1P + 11% 3d9 5d 3P
	-	269599.0	-	100% 3d9 5g 3D
	-	271365.0	-	67% 3d9 6d 3S + 24% 3d9 6d 3P + 10% 3d9 6d 1P
	-	271665.0	-	49% 3d9 6d 1P + 28% 3d9 6d 3D + 22% 3d9 6d 3P
	-	273910.0	-	98% 3d9 7s 3D
	-	274218.0	-	43% 3d9 6d 3P + 33% 3d9 6d 3S + 24% 3d9 6d 1P
	-	274452.0	-	71% 3d9 6d 3D + 16% 3d9 6d 1P + 11% 3d9 6d 3P
	-	281726.0	-	100% 3d9 6g 3D
	-	285428.0	-	100% 3d9 8s 3D
	-	289044.0	-	100% 3d9 7g 3D
	-	292406.0	-	100% 3d9 9s 3D
	-	293795.0	-	100% 3d9 8g 3D
2	79273.6	79284.0	-10.4	84% 3d9 4s 3D + 16% 3d9 4s 1D
	83500.3	83211.0	289.3	84% 3d9 4s 1D + 16% 3d9 4s 3D
	194303.3	194171.0	132.3	98% 3d8 4s2 <2>3F
	208041.3	207932.0	109.3	76% 3d8 4s2 <2>1D + 20% 3d8 4s2 <2>3P
	211725.5	211972.0	-246.5	73% 3d8 4s2 <2>3P + 20% 3d8 4s2 <2>1D + 6% 3d9 4d 3P
	215340.5	215305.0	35.5	53% 3d9 5s 3D + 47% 3d9 5s 1D
	217073.8	217300.0	-226.2	60% 3d9 4d 3P + 30% 3d9 4d 3D + 5% 3d8 4s2 <2>3P
	217846.8	217861.0	-14.2	36% 3d9 5s 1D + 33% 3d9 5s 3D + 12% 3d9 4d 1D + 9% 3d9 4d 3P
	218540.3	218385.0	155.3	27% 3d9 4d 3D + 25% 3d9 4d 1D + 15% 3d9 5s 1D + 14% 3d9 5s 3D
	220668.3	220581.0	87.3	36% 3d9 4d 3D + 28% 3d9 4d 1D + 19% 3d9 4d 3F + 15% 3d9 4d 3P
	221343.6	221211.0	132.6	64% 3d9 4d 3F + 33% 3d9 4d 1D
	-	250272.0	-	54% 3d9 6s 1D + 45% 3d9 6s 3D
	-	250935.0	-	68% 3d9 5d 3P + 29% 3d9 5d 3D
	-	251423.0	-	50% 3d9 5d 1D + 24% 3d9 5d 3D + 18% 3d9 5d 3F + 8% 3d9 5d 3P
	-	252975.0	-	54% 3d9 6s 3D + 45% 3d9 6s 1D
	-	253914.0	-	47% 3d9 5d 3D + 22% 3d9 5d 1D + 22% 3d9 5d 3P + 9% 3d9 5d 3F
	-	254202.0	-	71% 3d9 5d 3F + 26% 3d9 5d 1D
	-	269600.0	-	61% 3d9 5g 3D + 39% 3d9 5g 1D
	-	269648.0	-	65% 3d9 5g 3F + 22% 3d9 5g 1D + 13% 3d9 5g 3D
	-	271263.0	-	57% 3d9 7s 1D + 42% 3d9 7s 3D
	-	271681.0	-	65% 3d9 6d 3P + 31% 3d9 6d 3D
	-	271938.0	-	54% 3d9 6d 1D + 20% 3d9 6d 3D + 18% 3d9 6d 3F

				+ 8% 3d9 6d 3P
	-	272360.0	-	39% 3d9 5g 1D + 35% 3d9 5g 3F + 26% 3d9 5g 3D
	-	273976.0	-	57% 3d9 7s 3D + 42% 3d9 7s 1D
	-	274532.0	-	48% 3d9 6d 3D + 24% 3d9 6d 3P + 19% 3d9 6d 1D
				+ 8% 3d9 6d 3F
	-	274681.0	-	72% 3d9 6d 3F + 25% 3d9 6d 1D
	-	281727.0	-	61% 3d9 6g 3D + 39% 3d9 6g 1D
	-	281755.0	-	66% 3d9 6g 3F + 22% 3d9 6g 1D + 12% 3d9 6g 3D
	-	282742.0	-	59% 3d9 8s 1D + 41% 3d9 8s 3D
	-	284477.0	-	40% 3d9 6g 1D + 34% 3d9 6g 3F + 26% 3d9 6g 3D
	-	285461.0	-	59% 3d9 8s 3D + 41% 3d9 8s 1D
	-	289045.0	-	61% 3d9 7g 3D + 39% 3d9 7g 1D
	-	289063.0	-	66% 3d9 7g 3F + 22% 3d9 7g 1D + 12% 3d9 7g 3D
	-	289702.0	-	59% 3d9 9s 1D + 41% 3d9 9s 3D
	-	291790.0	-	40% 3d9 7g 1D + 34% 3d9 7g 3F + 27% 3d9 7g 3D
	-	292427.0	-	59% 3d9 9s 3D + 41% 3d9 9s 1D
	-	293795.0	-	62% 3d9 8g 3D + 38% 3d9 8g 1D
	-	293807.0	-	66% 3d9 8g 3F + 22% 3d9 8g 1D + 12% 3d9 8g 3D
	-	296537.0	-	40% 3d9 8g 1D + 34% 3d9 8g 3F + 27% 3d9 8g 3D
3	78096.3	78149.0	-52.7	100% 3d9 4s 3D
	192763.7	192651.0	112.7	100% 3d8 4s2 <2>3F
	214878.0	214921.0	-43.0	99% 3d9 5s 3D
	217655.8	217638.0	17.8	87% 3d9 4d 3D + 9% 3d9 4d 3F
	218040.9	218009.0	31.9	38% 3d9 4d 1F + 37% 3d9 4d 3G + 25% 3d9 4d 3F
	219684.9	219690.0	-5.1	63% 3d9 4d 3G + 23% 3d9 4d 1F + 14% 3d9 4d 3F
	221143.7	221023.0	120.7	53% 3d9 4d 3F + 35% 3d9 4d 1F + 12% 3d9 4d 3D
	-	250100.0	-	98% 3d9 6s 3D
	-	251176.0	-	82% 3d9 5d 3D + 12% 3d9 5d 3F + 4% 3d9 5d 1F
	-	251360.0	-	51% 3d9 5d 1F + 33% 3d9 5d 3F + 16% 3d9 5d 3G
	-	253578.0	-	84% 3d9 5d 3G + 10% 3d9 5d 1F + 6% 3d9 5d 3F
	-	254143.0	-	49% 3d9 5d 3F + 35% 3d9 5d 1F + 16% 3d9 5d 3D
	-	269648.0	-	38% 3d9 5g 3F + 35% 3d9 5g 3D + 28% 3d9 5g 1F
	-	269695.0	-	44% 3d9 5g 3G + 32% 3d9 5g 1F + 24% 3d9 5g 3F
	-	271174.0	-	99% 3d9 7s 3D
	-	271802.0	-	80% 3d9 6d 3D + 14% 3d9 6d 3F + 5% 3d9 6d 1F
	-	271898.0	-	53% 3d9 6d 1F + 34% 3d9 6d 3F + 13% 3d9 6d 3G
	-	272360.0	-	65% 3d9 5g 3D + 20% 3d9 5g 3F + 15% 3d9 5g 1F
	-	272435.0	-	56% 3d9 5g 3G + 25% 3d9 5g 1F + 19% 3d9 5g 3F
	-	274364.0	-	87% 3d9 6d 3G + 8% 3d9 6d 1F + 5% 3d9 6d 3F
	-	274650.0	-	48% 3d9 6d 3F + 34% 3d9 6d 1F + 18% 3d9 6d 3D
	-	281755.0	-	38% 3d9 6g 3F + 34% 3d9 6g 3D + 28% 3d9 6g 1F
	-	281782.0	-	44% 3d9 6g 3G + 32% 3d9 6g 1F + 24% 3d9 6g 3F
	-	282693.0	-	100% 3d9 8s 3D
	-	284476.0	-	66% 3d9 6g 3D + 19% 3d9 6g 3F + 15% 3d9 6g 1F
	-	284520.0	-	56% 3d9 6g 3G + 25% 3d9 6g 1F + 19% 3d9 6g 3F
	-	289063.0	-	38% 3d9 7g 3F + 34% 3d9 7g 3D + 28% 3d9 7g 1F
	-	289080.0	-	45% 3d9 7g 3G + 32% 3d9 7g 1F + 24% 3d9 7g 3F
	-	289671.0	-	100% 3d9 9s 3D
	-	291789.0	-	66% 3d9 7g 3D + 19% 3d9 7g 3F + 15% 3d9 7g 1F
	-	291817.0	-	55% 3d9 7g 3G + 26% 3d9 7g 1F + 19% 3d9 7g 3F
	-	293807.0	-	38% 3d9 8g 3F + 34% 3d9 8g 3D + 28% 3d9 8g 1F
	-	293818.0	-	45% 3d9 8g 3G + 32% 3d9 8g 1F + 24% 3d9 8g 3F
	-	296536.0	-	66% 3d9 8g 3D + 19% 3d9 8g 3F + 14% 3d9 8g 1F
	-	296555.0	-	55% 3d9 8g 3G + 26% 3d9 8g 1F + 19% 3d9 8g 3F
4	190341.3	190271.0	70.3	99% 3d8 4s2 <2>3F
	216464.0	216090.0	374.0	49% 3d9 4d 1G + 30% 3d8 4s2 <2>1G + 21% 3d9 4d 3G
	218041.5	217783.0	258.5	53% 3d9 4d 3G + 26% 3d9 4d 3F + 19% 3d8 4s2 <2>1G
	219360.5	218766.0	594.5	60% 3d9 4d 3F + 28% 3d8 4s2 <2>1G + 7% 3d9 4d 3G
				+ 5% 3d9 4d 1G
	221052.2	220504.0	548.2	45% 3d9 4d 1G + 23% 3d8 4s2 <2>1G + 19% 3d9 4d 3G
				+ 14% 3d9 4d 3F
	-	250878.0	-	52% 3d9 5d 3G + 48% 3d9 5d 1G
	-	251417.0	-	84% 3d9 5d 3F + 11% 3d9 5d 1G + 5% 3d9 5d 3G
	-	253709.0	-	44% 3d9 5d 3G + 41% 3d9 5d 1G + 15% 3d9 5d 3F
	-	269695.0	-	56% 3d9 5g 3F + 25% 3d9 5g 3G + 19% 3d9 5g 1G
	-	269723.0	-	40% 3d9 5g 1G + 32% 3d9 5g 3G + 28% 3d9 5g 3H
	-	271652.0	-	50% 3d9 6d 1G + 49% 3d9 6d 3G
	-	271925.0	-	87% 3d9 6d 3F + 9% 3d9 6d 1G
	-	272436.0	-	44% 3d9 5g 3F + 31% 3d9 5g 3G + 25% 3d9 5g 1G

		-	272461.0	-	72%	3d9	5g	3H	+	15%	3d9	5g	1G	+	12%	3d9	5g	3G
		-	274431.0	-	47%	3d9	6d	3G	+	41%	3d9	6d	1G	+	12%	3d9	6d	3F
		-	281782.0	-	56%	3d9	6g	3F	+	25%	3d9	6g	3G	+	19%	3d9	6g	1G
		-	281798.0	-	40%	3d9	6g	1G	+	32%	3d9	6g	3G	+	28%	3d9	6g	3H
		-	284520.0	-	44%	3d9	6g	3F	+	31%	3d9	6g	3G	+	25%	3d9	6g	1G
		-	284535.0	-	72%	3d9	6g	3H	+	16%	3d9	6g	1G	+	12%	3d9	6g	3G
		-	289080.0	-	55%	3d9	7g	3F	+	25%	3d9	7g	3G	+	19%	3d9	7g	1G
		-	289090.0	-	40%	3d9	7g	1G	+	32%	3d9	7g	3G	+	28%	3d9	7g	3H
		-	291817.0	-	45%	3d9	7g	3F	+	31%	3d9	7g	3G	+	24%	3d9	7g	1G
		-	291826.0	-	72%	3d9	7g	3H	+	16%	3d9	7g	1G	+	12%	3d9	7g	3G
		-	293818.0	-	55%	3d9	8g	3F	+	25%	3d9	8g	3G	+	19%	3d9	8g	1G
		-	293825.0	-	41%	3d9	8g	1G	+	31%	3d9	8g	3G	+	28%	3d9	8g	3H
		-	296555.0	-	45%	3d9	8g	3F	+	31%	3d9	8g	3G	+	24%	3d9	8g	1G
		-	296561.0	-	72%	3d9	8g	3H	+	16%	3d9	8g	1G	+	12%	3d9	8g	3G
5	216607.4	216699.0	-91.6	100%	3d9	4d	3G											
		-	250798.0	-	100%	3d9	5d	3G										
		-	269715.0	-	46%	3d9	5g	1H	+	40%	3d9	5g	3H	+	14%	3d9	5g	3I
		-	269723.0	-	72%	3d9	5g	3G	+	14%	3d9	5g	3H	+	13%	3d9	5g	1H
		-	271614.0	-	100%	3d9	6d	3G										
		-	272386.0	-	86%	3d9	5g	3I	+	8%	3d9	5g	1H	+	6%	3d9	5g	3H
		-	272462.0	-	39%	3d9	5g	3H	+	33%	3d9	5g	1H	+	28%	3d9	5g	3G
		-	281794.0	-	47%	3d9	6g	1H	+	39%	3d9	6g	3H	+	14%	3d9	6g	3I
		-	281798.0	-	72%	3d9	6g	3G	+	15%	3d9	6g	3H	+	13%	3d9	6g	1H
		-	284491.0	-	86%	3d9	6g	3I	+	8%	3d9	6g	1H	+	6%	3d9	6g	3H
		-	284535.0	-	39%	3d9	6g	3H	+	33%	3d9	6g	1H	+	28%	3d9	6g	3G
		-	289087.0	-	47%	3d9	7g	1H	+	39%	3d9	7g	3H	+	14%	3d9	7g	3I
		-	289090.0	-	72%	3d9	7g	3G	+	15%	3d9	7g	3H	+	13%	3d9	7g	1H
		-	291799.0	-	86%	3d9	7g	3I	+	7%	3d9	7g	1H	+	6%	3d9	7g	3H
		-	291826.0	-	39%	3d9	7g	3H	+	33%	3d9	7g	1H	+	28%	3d9	7g	3G
		-	293823.0	-	47%	3d9	8g	1H	+	39%	3d9	8g	3H	+	14%	3d9	8g	3I
		-	293825.0	-	72%	3d9	8g	3G	+	15%	3d9	8g	3H	+	13%	3d9	8g	1H
		-	296543.0	-	86%	3d9	8g	3I	+	7%	3d9	8g	1H	+	6%	3d9	8g	3H
		-	296561.0	-	39%	3d9	8g	3H	+	33%	3d9	8g	1H	+	28%	3d9	8g	3G
6		-	269638.0	-	54%	3d9	5g	1I	+	46%	3d9	5g	3I					
		-	269716.0	-	86%	3d9	5g	3H	+	8%	3d9	5g	3I	+	7%	3d9	5g	1I
		-	272386.0	-	46%	3d9	5g	3I	+	40%	3d9	5g	1I	+	14%	3d9	5g	3H
		-	281749.0	-	54%	3d9	6g	1I	+	46%	3d9	6g	3I					
		-	281794.0	-	86%	3d9	6g	3H	+	7%	3d9	6g	3I	+	6%	3d9	6g	1I
		-	284491.0	-	46%	3d9	6g	3I	+	40%	3d9	6g	1I	+	14%	3d9	6g	3H
		-	289059.0	-	54%	3d9	7g	1I	+	46%	3d9	7g	3I					
		-	289087.0	-	86%	3d9	7g	3H	+	7%	3d9	7g	3I	+	6%	3d9	7g	1I
		-	291799.0	-	47%	3d9	7g	3I	+	40%	3d9	7g	1I	+	14%	3d9	7g	3H
		-	293804.0	-	54%	3d9	8g	1I	+	46%	3d9	8g	3I					
		-	293823.0	-	86%	3d9	8g	3H	+	7%	3d9	8g	3I	+	6%	3d9	8g	1I
		-	296543.0	-	47%	3d9	8g	3I	+	40%	3d9	8g	1I	+	14%	3d9	8g	3H
7		-	269639.0	-	100%	3d9	5g	3I										
		-	281749.0	-	100%	3d9	6g	3I										
		-	289059.0	-	100%	3d9	7g	3I										
		-	293804.0	-	100%	3d9	8g	3I										

Table II.

Observed and least squares fitted energy levels of odd parity configuration of Zn III in Cm^{-1} :

J	E(obs)	E(LSF)	diff.	LS-composition.
1				
0	141392.5	141393.0	-0.5	100% 3d9 4p 3P
	-	227920.0	-	95% 3d8 4s 4p ((<2>3F)4F)5D + 5% 3d8 4s 4p ((<2>3P)4F)5D
	236560.0	236569.0	-9.0	100% 3d9 5p 3P
	-	247320.0	-	67% 3d8 4s 4p ((<2>1D)2D)3P + 19% 3d8 4s 4p ((<2>3P)2P)3P
				+ 11% 3d8 4s 4p ((<2>3P)4P)3P
	-	249961.0	-	93% 3d8 4s 4p ((<2>3P)4P)5D + 5% 3d8 4s 4p ((<2>3F)4F)5D
	-	254121.0	-	51% 3d8 4s 4p ((<2>3P)2P)3P + 29% 3d8 4s 4p ((<2>1D)2D)3P
				+ 17% 3d8 4s 4p ((<2>3P)4P)3P
	257491.1	257438.0	53.1	99% 3d9 4f 3P
	-	260653.0	-	98% 3d8 4s 4p ((<2>3P)2P)1S
	270830.0	270328.0	502.0	98% 3d9 6p 3P
	-	278531.0	-	63% 3d8 4s 4p ((<2>3P)4P)3P + 26% 3d8 4s 4p ((<2>3P)2P)3P
				+ 9% 3d9 5f 3P
	-	280453.0	-	91% 3d9 5f 3P + 6% 3d8 4s 4p ((<2>3P)4P)3P
	-	296668.0	-	98% 3d8 4s 4p ((<0>1S)2S)3P
1	140071.0	140067.0	4.0	97% 3d9 4p 3P
	147571.2	147446.0	125.2	94% 3d9 4p 3D + 5% 3d9 4p 1P
	147498.6	147571.0	-72.4	94% 3d9 4p 1P
	-	227386.0	-	93% 3d8 4s 4p ((<2>3F)4F)5D + 4% 3d8 4s 4p ((<2>3P)4P)5D
	-	230771.0	-	95% 3d8 4s 4p ((<2>3F)4F)5F
	-	234072.0	-	55% 3d8 4s 4p ((<2>3F)2F)3D + 28% 3d8 4s 4p ((<2>3F)4F)3D
				+ 4% 3d9 5p 3D
	234866.9	234847.0	19.9	67% 3d9 5p 3P + 23% 3d9 5p 1P
				+ 4% 3d9 5p 3D
	237506.8	237461.0	45.8	72% 3d9 5p 1P + 27% 3d9 5p 3P
	238205.5	238064.0	141.5	89% 3d9 5p 3D + 4% 3d9 5p 1P
	-	244271.0	-	87% 3d8 4s 4p ((<2>3P)4P)5P + 6% 3d8 4s 4p ((<2>1D)2D)3P
	-	246472.0	-	73% 3d8 4s 4p ((<2>1D)2D)3D + 8% 3d8 4s 4p ((<2>3P)4P)5P
				+ 6% 3d8 4s 4p ((<2>3F)2F)3D + 4% 3d8 4s 4p ((<2>1D)2D)3P
	-	248140.0	-	63% 3d8 4s 4p ((<2>1D)2D)3P + 12% 3d8 4s 4p ((<2>1D)2D)3D
				+ 10% 3d8 4s 4p ((<2>3P)2P)3P + 6% 3d8 4s 4p ((<2>3P)4P)3P
	-	249967.0	-	92% 3d8 4s 4p ((<2>3P)4P)5D + 4% 3d8 4s 4p ((<2>3F)4F)5D
	-	253270.0	-	43% 3d8 4s 4p ((<2>3P)2P)3P + 17% 3d8 4s 4p ((<2>1D)2D)3P
				+ 15% 3d8 4s 4p ((<2>3P)4P)3P + 10% 3d8 4s 4p ((<2>3P)2P)3D
	-	254325.0	-	51% 3d8 4s 4p ((<2>3P)2P)3D + 26% 3d8 4s 4p ((<2>3P)4P)3D
				+ 6% 3d8 4s 4p ((<2>3P)2P)3P + 5% 3d8 4s 4p ((<2>3P)2P)1P
	-	256079.0	-	82% 3d8 4s 4p ((<2>3P)2P)1P + 4% 3d8 4s 4p ((<2>3P)2P)3P
	257566.1	257510.0	56.1	80% 3d9 4f 3P + 16% 3d9 4f 3D
	257908.2	257854.0	54.2	49% 3d9 4f 1P + 44% 3d9 4f 3D
	-	258758.0	-	57% 3d8 4s 4p ((<2>3P)2P)3S + 41% 3d8 4s 4p ((<2>3P)4P)3S
	260584.1	260522.0	62.1	44% 3d9 4f 1P + 38% 3d9 4f 3D
				+ 16% 3d9 4f 3P
	-	261537.0	-	59% 3d8 4s 4p ((<2>3F)4F)3D + 28% 3d8 4s 4p ((<2>3F)2F)3D
				+ 5% 3d8 4s 4p ((<2>3P)4P)3D
	-	269720.0	-	72% 3d9 6p 3P + 19% 3d9 6p 1P
				+ 6% 3d9 6p 3D
	-	270741.0	-	83% 3d9 6p 3D + 12% 3d9 6p 3P
	-	270777.0	-	76% 3d9 6p 1P + 14% 3d9 6p 3P
				+ 8% 3d9 6p 3D
	-	277155.0	-	40% 3d8 4s 4p ((<2>3P)4P)3P + 34% 3d8 4s 4p ((<2>1D)2D)1P
				+ 17% 3d8 4s 4p ((<2>3P)2P)3P
	-	279737.0	-	52% 3d8 4s 4p ((<2>1D)2D)1P + 21% 3d8 4s 4p ((<2>3P)4P)3P
				+ 11% 3d9 5f 3P + 9% 3d8 4s 4p ((<2>3P)2P)3P
	-	280439.0	-	52% 3d9 5f 3D + 22% 3d9 5f 3P
				+ 8% 3d9 5f 1P + 5% 3d8 4s 4p ((<2>3P)4P)3P
	280501.0	280500.0	1.0	47% 3d9 5f 3P + 43% 3d9 5f 1P
				+ 5% 3d9 5f 3D
	-	282256.0	-	51% 3d8 4s 4p ((<2>3P)4P)3D + 29% 3d8 4s 4p ((<2>3P)2P)3D
				+ 11% 3d9 5f 1P
	-	283364.0	-	40% 3d9 5f 3D + 36% 3d9 5f 1P
				+ 15% 3d9 5f 3P + 5% 3d8 4s 4p ((<2>3P)4P)3D

	-	286659.0	-	57% 3d8 4s 4p ((<2>3P)4P)3S + 41% 3d8 4s 4p ((<2>3P)2P)3S
	-	297161.0	-	98% 3d8 4s 4p ((<0>1S)2S)3P
	-	326878.0	-	99% 3d8 4s 4p ((<0>1S)2S)1P
2	137866.4	137889.0	-22.6	97% 3d9 4p 3P
	142483.3	142528.0	-44.7	94% 3d9 4p 3F + 5% 3d9 4p 3D
	145243.9	145317.0	-73.1	58% 3d9 4p 1D + 36% 3d9 4p 3D
				+ 5% 3d9 4p 3F
	147921.5	147999.0	-77.5	57% 3d9 4p 3D + 41% 3d9 4p 1D
	-	226345.0	-	90% 3d8 4s 4p ((<2>3F)4F)5D + 4% 3d8 4s 4p ((<2>3F)4F)5F
	-	228145.0	-	94% 3d8 4s 4p ((<2>3F)4F)5G + 4% 3d8 4s 4p ((<2>3F)4F)5F
	-	230458.0	-	88% 3d8 4s 4p ((<2>3F)4F)5F + 5% 3d8 4s 4p ((<2>3F)4F)5G
	-	232739.0	-	48% 3d8 4s 4p ((<2>3F)2F)3D + 24% 3d8 4s 4p ((<2>3F)4F)3D
				+ 6% 3d8 4s 4p ((<2>3F)2F)3F + 5% 3d8 4s 4p ((<2>3F)2F)1D
	233610.4	233516.0	94.4	90% 3d9 5p 3P + 5% 3d9 5p 3D
	-	234901.0	-	24% 3d9 5p 1D + 23% 3d8 4s 4p ((<2>3F)2F)3F
				+ 15% 3d9 5p 3D + 15% 3d9 5p 3F
	235452.5	235654.0	-201.5	28% 3d8 4s 4p ((<2>3F)2F)3F + 28% 3d9 5p 1D
				+ 16% 3d8 4s 4p ((<2>3F)4F)3F + 11% 3d8 4s 4p ((<2>3F)2F)3D
	-	236758.0	-	61% 3d9 5p 3F + 21% 3d8 4s 4p ((<2>3F)2F)1D
				+ 10% 3d9 5p 1D
	237047.8	237411.0	-363.2	44% 3d8 4s 4p ((<2>3F)2F)1D + 29% 3d9 5p 3D
				+ 22% 3d9 5p 3F
	-	238538.0	-	36% 3d9 5p 1D + 35% 3d9 5p 3D
				+ 21% 3d8 4s 4p ((<2>3F)2F)1D
	-	243715.0	-	77% 3d8 4s 4p ((<2>3P)4P)5P + 8% 3d8 4s 4p ((<2>1D)2D)3D
				+ 7% 3d8 4s 4p ((<2>1D)2D)3P
	-	245983.0	-	77% 3d8 4s 4p ((<2>1D)2D)3F + 8% 3d8 4s 4p ((<2>1D)2D)3D
	-	246955.0	-	67% 3d8 4s 4p ((<2>1D)2D)3D + 11% 3d8 4s 4p ((<2>3P)4P)5P
				+ 10% 3d8 4s 4p ((<2>1D)2D)3F
	-	248771.0	-	80% 3d8 4s 4p ((<2>1D)2D)3P + 6% 3d8 4s 4p ((<2>3P)4P)5P
				+ 5% 3d8 4s 4p ((<2>1D)2D)3D
	-	250014.0	-	90% 3d8 4s 4p ((<2>3P)4P)5D
	-	252561.0	-	55% 3d8 4s 4p ((<2>3P)2P)3P + 22% 3d8 4s 4p ((<2>3P)4P)3P
				+ 8% 3d8 4s 4p ((<2>3P)2P)3D + 5% 3d8 4s 4p ((<2>1D)2D)3P
	-	254096.0	-	42% 3d8 4s 4p ((<2>3P)2P)3D + 22% 3d8 4s 4p ((<2>3P)4P)3D
				+ 9% 3d8 4s 4p ((<2>3P)2P)1D + 7% 3d8 4s 4p ((<2>3P)2P)3P
	-	255739.0	-	95% 3d8 4s 4p ((<2>3P)4P)5S
	-	256204.0	-	78% 3d8 4s 4p ((<2>1G)2G)3F + 5% 3d8 4s 4p ((<2>1D)2D)3F
				+ 4% 3d8 4s 4p ((<2>3P)2P)3D
	-	256987.0	-	64% 3d8 4s 4p ((<2>3P)2P)1D + 13% 3d9 4f 1D
				+ 6% 3d8 4s 4p ((<2>1G)2G)3F + 5% 3d9 4f 3P
	-	257686.0	-	48% 3d9 4f 3D + 35% 3d9 4f 3P
				+ 7% 3d8 4s 4p ((<2>3P)2P)1D + 6% 3d9 4f 3F
	-	257887.0	-	44% 3d9 4f 1D + 30% 3d9 4f 3F
				+ 12% 3d8 4s 4p ((<2>3P)2P)1D + 7% 3d9 4f 3D
	-	260098.0	-	47% 3d8 4s 4p ((<2>3F)4F)3D + 21% 3d8 4s 4p ((<2>3F)2F)3D
				+ 12% 3d9 4f 3P + 6% 3d8 4s 4p ((<2>3P)4P)3D
	260418.1	260409.0	9.1	42% 3d9 4f 3P + 24% 3d9 4f 3D
				+ 15% 3d9 4f 1D + 12% 3d8 4s 4p ((<2>3F)4F)3D
	260805.9	260645.0	160.9	60% 3d9 4f 3F + 23% 3d9 4f 1D
				+ 14% 3d9 4f 3D
	-	263277.0	-	58% 3d8 4s 4p ((<2>3F)4F)3F + 31% 3d8 4s 4p ((<2>3F)2F)3F
	269027.0	269228.0	-201.0	91% 3d9 6p 3P + 6% 3d9 6p 3D
	269863.0	269568.0	295.0	70% 3d9 6p 1D + 23% 3d9 6p 3D
				+ 5% 3d9 6p 3F
	269863.0	270373.0	-510.0	80% 3d9 6p 3F + 13% 3d9 6p 1D
				+ 4% 3d9 6p 3D
	-	270719.0	-	65% 3d9 6p 3D + 14% 3d9 6p 3F
				+ 14% 3d9 6p 1D + 5% 3d9 6p 3P
	-	275494.0	-	63% 3d8 4s 4p ((<2>1D)2D)1D + 20% 3d8 4s 4p ((<2>3P)4P)3P
				+ 9% 3d8 4s 4p ((<2>3P)2P)3P
	-	278609.0	-	45% 3d8 4s 4p ((<2>3P)4P)3P + 29% 3d8 4s 4p ((<2>1D)2D)1D
				+ 21% 3d8 4s 4p ((<2>3P)2P)3P
	-	280362.0	-	56% 3d9 5f 3D + 25% 3d9 5f 3P
				+ 8% 3d9 5f 3F + 4% 3d8 4s 4p ((<2>3P)4P)3D
	-	280514.0	-	57% 3d9 5f 1D + 27% 3d9 5f 3F
				+ 13% 3d9 5f 3P
	-	281829.0	-	50% 3d8 4s 4p ((<2>3P)4P)3D + 31% 3d8 4s 4p ((<2>3P)2P)3D
				+ 8% 3d9 5f 3P + 7% 3d9 5f 3F
	-	283206.0	-	49% 3d9 5f 3P + 28% 3d9 5f 1D

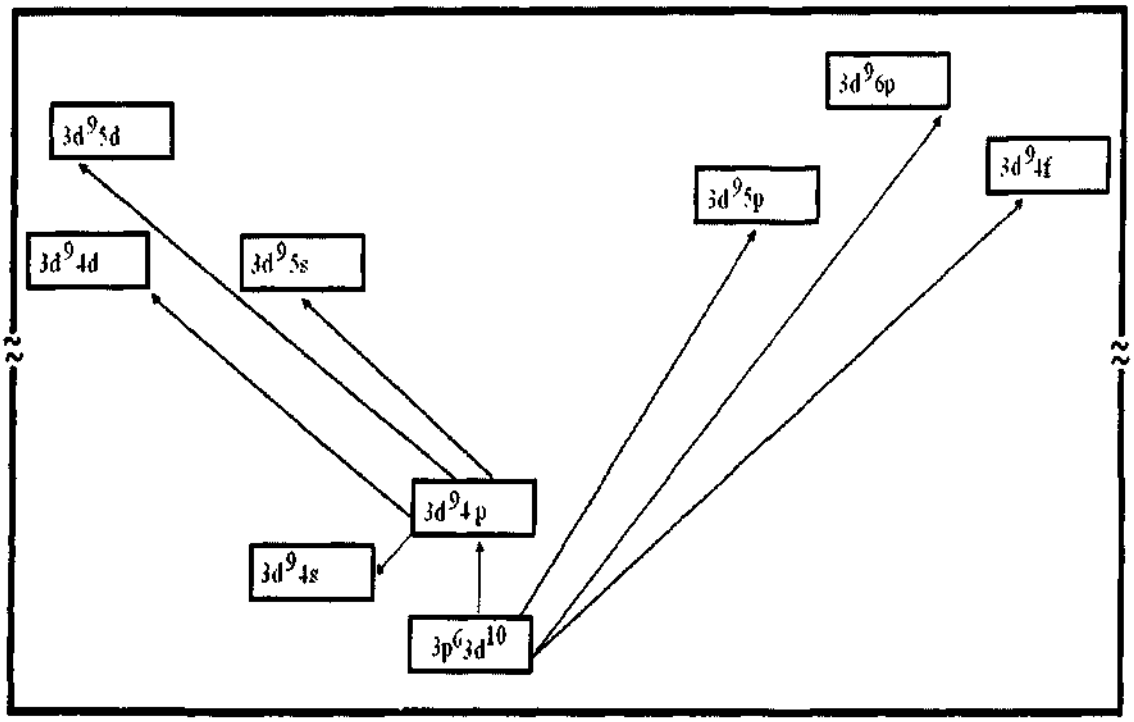

Figure (8.1): Grotorian diagram of Zn III (not to the scale)

(8.4) Conversion of spectrum image into relative intensity versus pixel number plot :

The CCD devices are used in imaging. A CCD device image sensor is an analog integrated circuit that converts an optical image into an electronic output. The charge-coupled devices are one or two dimensional array of metal-oxide-semiconductor (MOS) photo-capacitors. The charge introduced on a photo-capacitor is proportional to the number of absorbing photons (400 nm $<\lambda<$ 1100 nm). Now a day's CCDs are used in spectroscopy similar to that of photographic plates. The CCD detectors designed for the use of scanners and cameras are not required to be cooled below room temperature. Typically, scanners use 8-bit digitizers allowing a 256 level gray scale for measurement of light intensity.

An image recorded on a photo-scanner may be thought as three dimensional representation of the image. Each pixel of the image shows charge on a photo-capacitor. The white pixel has a high value of 255 and black pixel a low value of intensity i.e. zero, with eight bit resolution. The spectrum is represented as intensity versus wavelength, so the image has to be transformed into two dimensional representations. If the spectrum is

spread in horizontal direction then each row contains the same data. The transformation of three dimensional image to two dimensional representations is achieved by summing the intensity values of the pixels in each column of the image to remove the redundancy of data.

To do this transformation, the image is saved in standard file format (BMP) then we use software to read and sum the intensity values for each pixel in a column to convert the image to intensity versus column number. A software IM2SPEC do this image conversion for data stored in the bitmap file format i.e. BMP. The IM2SPEC program converts a BITMAP image file to an ASCII "relative intensity" versus "horizontal pixel number" [20]. The same conversion of image into spectrum can be accomplice by writing a simple programme in MathCAD with inbuilt function READBMP. The numbers of pixel can be converted into wavelengths.

The wavelength of an emission line converted to two dimensional representation can be estimated by its peak location in pixel position/number displayed. Few standard known lines of the spectrum can be used to calibrate the spectrum and to calculate the plate factor like quantity $\frac{\Delta\lambda}{\Delta Pixel}$.The quantity $\Delta pixel$ is the difference of two pixel number for the corresponding wavelengths. The particular pixel is assigned a wavelength on the basis of location line and these can be fit using a polynomial. Determining the wavelength of standard lines, this process is iterated until all the known lines can be accurately assigned.[21]

The Zinc spectrum (figure 7.8) was scanned on HP Scanjet G4010 photo-scanner at scan resolution of 2400 ppi with BMP file format. The scanned image is first inverted by using the Microsoft paint, the scanned image of the spectrum was read by the MathCAD using READBMP function. The plot between intensity versus pixel number is shown in figure (8.2). The following is the MathCad programme.

name := "sample.bmp"

M := READBMP(name)

i_{max} := cols(M) − 1

j_{max} := rows(M) − 1

i := 0.. i_{max} j_{max} =

$$\text{Intensity}_i := \sum_{j=0}^{j_{max}} M_{j,i}$$

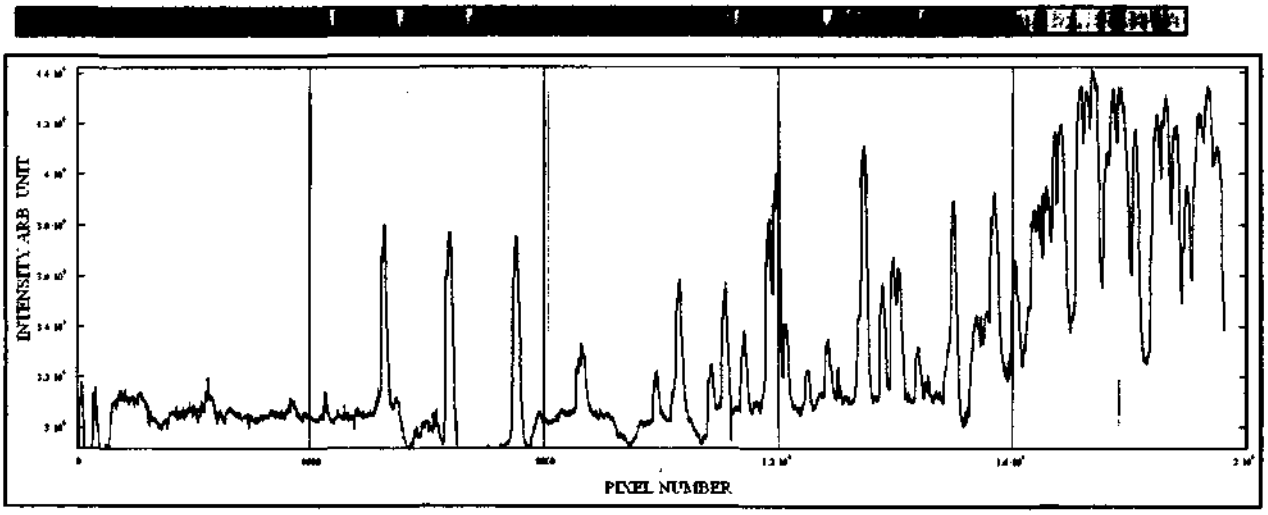

Figure (8.2): Plot between intensity versus pixel number

				+ 14% 3d9 5f 3D + 6% 3d9 5f 3F
	-	283345.0	-	52% 3d9 5f 3F + 27% 3d9 5f 3D
				+ 12% 3d9 5f 1D
	-	298199.0	-	99% 3d8 4s 4p ((<0>1S)2S)3P
3	140654.8	140658.0	-3.2	69% 3d9 4p 3F + 28% 3d9 4p 1F
	144501.2	144512.0	-10.8	59% 3d9 4p 1F + 26% 3d9 4p 3D
				+ 15% 3d9 4p 3F
	145966.6	145877.0	89.6	71% 3d9 4p 3D + 16% 3d9 4p 3F
				+ 13% 3d9 4p 1F
	-	224895.0	-	89% 3d8 4s 4p ((<2>3F)4F)5D + 5% 3d8 4s 4p ((<2>3F)4F)5F
	-	227397.0	-	85% 3d8 4s 4p ((<2>3F)4F)5G + 9% 3d8 4s 4p ((<2>3F)4F)5F
	-	229853.0	-	80% 3d8 4s 4p ((<2>3F)4F)5F + 10% 3d8 4s 4p ((<2>3F)4F)5G
	-	231868.0	-	50% 3d8 4s 4p ((<2>3F)2F)3D + 22% 3d8 4s 4p ((<2>3F)4F)3D
				+ 9% 3d8 4s 4p ((<2>3F)2F)3F + 4% 3d8 4s 4p ((<2>3F)4F)3F
	-	232597.0	-	53% 3d8 4s 4p ((<2>3F)2F)3G + 29% 3d8 4s 4p ((<2>3F)4F)3G
				+ 7% 3d8 4s 4p ((<2>3F)2F)3D
	-	233709.0	-	28% 3d9 5p 3F + 17% 3d9 5p 1F
				+ 16% 3d8 4s 4p ((<2>3F)2F)3F + 12% 3d8 4s 4p ((<2>3F)4F)3F
	234384.0	234599.0	-215.0	26% 3d9 5p 1F + 26% 3d9 5p 3F
				+ 20% 3d8 4s 4p ((<2>3F)2F)3F + 10% 3d8 4s 4p ((<2>3F)4F)3F
	235623.9	235461.0	162.9	77% 3d9 5p 3D + 14% 3d9 5p 1F
	-	237266.0	-	34% 3d8 4s 4p ((<2>3F)2F)1F + 25% 3d9 5p 3F
				+ 20% 3d9 5p 1F + 11% 3d9 5p 3D
	-	237957.0	-	41% 3d8 4s 4p ((<2>3F)2F)1F + 23% 3d9 5p 1F
				+ 19% 3d9 5p 3F + 8% 3d8 4s 4p ((<2>3F)2F)3F
	-	243751.0	-	76% 3d8 4s 4p ((<2>3P)4P)5P + 18% 3d8 4s 4p ((<2>1D)2D)3D
	-	246368.0	-	76% 3d8 4s 4p ((<2>1D)2D)3F + 6% 3d8 4s 4p ((<2>3P)4P)5D
				+ 6% 3d8 4s 4p ((<2>3P)4P)5P + 5% 3d8 4s 4p ((<2>1G)2G)3F
	-	247634.0	-	72% 3d8 4s 4p ((<2>1D)2D)3D + 16% 3d8 4s 4p ((<2>3P)4P)5P
				+ 4% 3d8 4s 4p ((<2>1D)2D)3F
	-	250163.0	-	84% 3d8 4s 4p ((<2>3P)4P)5D + 7% 3d8 4s 4p ((<2>1D)2D)3F
	-	254166.0	-	49% 3d8 4s 4p ((<2>3P)2P)3D + 27% 3d8 4s 4p ((<2>3P)4P)3D
				+ 9% 3d8 4s 4p ((<2>1G)2G)3F + 8% 3d8 4s 4p ((<2>3F)4F)3D
	-	255860.0	-	75% 3d8 4s 4p ((<2>1G)2G)3F + 9% 3d8 4s 4p ((<2>1D)2D)3F
				+ 5% 3d8 4s 4p ((<2>3P)2P)3D + 4% 3d8 4s 4p ((<2>3F)2F)3F
	-	257669.0	-	38% 3d9 4f 3D + 21% 3d8 4s 4p ((<2>3F)4F)3D
				+ 17% 3d9 4f 3F + 9% 3d8 4s 4p ((<2>3F)2F)3D
	-	257892.0	-	45% 3d9 4f 1F + 27% 3d9 4f 3G
				+ 20% 3d9 4f 3F
	258075.7	258098.0	-22.3	38% 3d8 4s 4p ((<2>3F)4F)3D + 23% 3d9 4f 3D
				+ 16% 3d8 4s 4p ((<2>3F)2F)3D + 12% 3d9 4f 3F
	-	259888.0	-	35% 3d8 4s 4p ((<2>3F)4F)3G + 19% 3d8 4s 4p ((<2>3F)2F)3G
				+ 17% 3d9 4f 3G + 14% 3d9 4f 1F
	-	260594.0	-	34% 3d9 4f 3D + 33% 3d9 4f 3F
				+ 23% 3d9 4f 1F + 5% 3d8 4s 4p ((<2>3F)4F)3F
	260981.9	261289.0	-307.1	48% 3d9 4f 3G + 14% 3d8 4s 4p ((<2>3F)4F)3G
				+ 10% 3d9 4f 1F + 10% 3d8 4s 4p ((<2>3F)4F)3F
	-	261969.0	-	91% 3d8 4s 4p ((<2>1G)2G)3G + 5% 3d8 4s 4p ((<2>3F)4F)3G
	-	262236.0	-	43% 3d8 4s 4p ((<2>3F)4F)3F + 25% 3d8 4s 4p ((<2>3F)2F)3F
				+ 7% 3d9 4f 3F + 6% 3d9 4f 3G
	269417.0	269422.0	-5.0	47% 3d9 6p 1F + 46% 3d9 6p 3F
				+ 5% 3d9 6p 3D
	-	269783.0	-	83% 3d9 6p 3D + 15% 3d9 6p 1F
	-	270588.0	-	52% 3d9 6p 3F + 36% 3d9 6p 1F
				+ 10% 3d9 6p 3D
	-	275861.0	-	82% 3d8 4s 4p ((<2>1D)2D)1F + 5% 3d8 4s 4p ((<2>3P)4P)3D
				+ 4% 3d8 4s 4p ((<2>1G)2G)1F
	-	280370.0	-	51% 3d9 5f 3D + 29% 3d9 5f 3F
				+ 9% 3d8 4s 4p ((<2>3P)4P)3D + 5% 3d8 4s 4p ((<2>3P)2P)3D
	-	280662.0	-	55% 3d9 5f 1F + 22% 3d9 5f 3G
				+ 15% 3d9 5f 3F + 7% 3d9 5f 3D
	-	281349.0	-	41% 3d8 4s 4p ((<2>3P)4P)3D + 28% 3d8 4s 4p ((<2>3P)2P)3D
				+ 13% 3d9 5f 3F + 4% 3d8 4s 4p ((<2>1D)2D)1F
	-	283360.0	-	41% 3d9 5f 3F + 32% 3d9 5f 3G
				+ 23% 3d9 5f 3D
	-	283416.0	-	43% 3d9 5f 3G + 37% 3d9 5f 1F
				+ 16% 3d9 5f 3D
	-	285607.0	-	89% 3d8 4s 4p ((<2>1G)2G)1F + 8% 3d8 4s 4p ((<2>1D)2D)1F
4	141327.0	141240.0	87.0	100% 3d9 4p 3F

	-	223182.0	-	93% 3d8 4s 4p ((<2>3F)4F)5D
	-	226494.0	-	77% 3d8 4s 4p ((<2>3F)4F)5G + 12% 3d8 4s 4p ((<2>3F)4F)5F
				+ 4% 3d8 4s 4p ((<2>3F)2F)3G
	-	228963.0	-	78% 3d8 4s 4p ((<2>3F)4F)5F + 11% 3d8 4s 4p ((<2>3F)4F)5G
	-	230958.0	-	39% 3d8 4s 4p ((<2>3F)2F)3G + 25% 3d8 4s 4p ((<2>3F)2F)1G
				+ 22% 3d8 4s 4p ((<2>3F)4F)3G + 11% 3d8 4s 4p ((<2>3F)4F)5G
	-	233516.0	-	44% 3d8 4s 4p ((<2>3F)2F)3F + 29% 3d8 4s 4p ((<2>3F)4F)3F
				+ 18% 3d9 5p 3F + 5% 3d8 4s 4p ((<2>3F)4F)5F
	234576.0	234643.0	-67.0	80% 3d9 5p 3F + 11% 3d8 4s 4p ((<2>3F)2F)3F
				+ 4% 3d8 4s 4p ((<2>3F)4F)3F
	-	235388.0	-	67% 3d8 4s 4p ((<2>3F)2F)1G + 16% 3d8 4s 4p ((<2>3F)2F)3G
				+ 11% 3d8 4s 4p ((<2>3F)4F)3G
	-	246760.0	-	71% 3d8 4s 4p ((<2>1D)2D)3F + 20% 3d8 4s 4p ((<2>3P)4P)5D
				+ 6% 3d8 4s 4p ((<2>1G)2G)3F
	-	250447.0	-	75% 3d8 4s 4p ((<2>3P)4P)5D + 15% 3d8 4s 4p ((<2>1D)2D)3F
				+ 8% 3d8 4s 4p ((<2>1G)2G)3F
	-	254301.0	-	99% 3d8 4s 4p ((<2>1G)2G)3H
	-	255203.0	-	74% 3d8 4s 4p ((<2>1G)2G)3F + 11% 3d8 4s 4p ((<2>1D)2D)3F
				+ 7% 3d8 4s 4p ((<2>3F)2F)3F + 4% 3d8 4s 4p ((<2>3F)4F)3F
	-	257541.0	-	40% 3d9 4f 3G + 19% 3d9 4f 3F
				+ 16% 3d8 4s 4p ((<2>3F)4F)3G + 9% 3d8 4s 4p ((<2>3F)2F)3G
	258239.6	257964.0	275.6	46% 3d9 4f 1G + 40% 3d9 4f 3F
				+ 7% 3d9 4f 3H
	258178.3	259007.0	-828.7	33% 3d8 4s 4p ((<2>3F)4F)3G + 21% 3d8 4s 4p ((<2>3F)2F)3G
				+ 19% 3d9 4f 3F + 8% 3d9 4f 3H
	-	259899.0	-	44% 3d8 4s 4p ((<2>3F)4F)3F + 24% 3d8 4s 4p ((<2>3F)2F)3F
				+ 9% 3d9 4f 1G + 9% 3d9 4f 3G
	260623.1	260544.0	79.1	79% 3d9 4f 3H + 16% 3d9 4f 1G
	260988.4	261182.0	-193.6	40% 3d9 4f 3G + 19% 3d9 4f 3F
				+ 18% 3d9 4f 1G + 7% 3d8 4s 4p ((<2>3F)4F)3G
	-	262096.0	-	97% 3d8 4s 4p ((<2>1G)2G)3G
	269499.0	269575.0	-76.0	99% 3d9 6p 3F
	-	280598.0	-	59% 3d9 5f 3F + 38% 3d9 5f 1G
	-	280615.0	-	51% 3d9 5f 3G + 21% 3d9 5f 1G
				+ 17% 3d9 5f 3F + 11% 3d9 5f 3H
	-	283181.0	-	86% 3d9 5f 3H + 9% 3d9 5f 1G
				+ 5% 3d9 5f 3G
	-	283364.0	-	43% 3d9 5f 3G + 32% 3d9 5f 1G
				+ 24% 3d9 5f 3F
	-	291145.0	-	100% 3d8 4s 4p ((<2>1G)2G)1G
5	-	225759.0	-	75% 3d8 4s 4p ((<2>3F)4F)5G + 19% 3d8 4s 4p ((<2>3F)4F)5F
	-	227848.0	-	80% 3d8 4s 4p ((<2>3F)4F)5F + 16% 3d8 4s 4p ((<2>3F)4F)5G
	-	231487.0	-	55% 3d8 4s 4p ((<2>3F)2F)3G + 36% 3d8 4s 4p ((<2>3F)4F)3G
				+ 9% 3d8 4s 4p ((<2>3F)4F)5G
	-	254810.0	-	98% 3d8 4s 4p ((<2>1G)2G)3H
	-	256280.0	-	48% 3d8 4s 4p ((<2>3F)4F)3G + 31% 3d8 4s 4p ((<2>3F)2F)3G
				+ 20% 3d9 4f 3G
	257796.0	257675.0	121.0	55% 3d9 4f 1H + 44% 3d9 4f 3H
	258171.2	258455.0	-283.8	62% 3d9 4f 3G + 11% 3d8 4s 4p ((<2>3F)4F)3G
				+ 9% 3d9 4f 3H + 8% 3d8 4s 4p ((<2>3F)2F)3G
	260613.1	260534.0	79.1	45% 3d9 4f 3H + 36% 3d9 4f 1H
				+ 18% 3d9 4f 3G
	-	262176.0	-	99% 3d8 4s 4p ((<2>1G)2G)3G
	-	280332.0	-	58% 3d9 5f 1H + 39% 3d9 5f 3H
	-	280622.0	-	85% 3d9 5f 3G + 12% 3d9 5f 3H
	-	282990.0	-	47% 3d9 5f 3H + 27% 3d9 5f 1H
				+ 14% 3d9 5f 3G + 13% 3d8 4s 4p ((<2>1G)2G)1H
	-	284494.0	-	84% 3d8 4s 4p ((<2>1G)2G)1H + 11% 3d9 5f 1H
6	-	225667.0	-	100% 3d8 4s 4p ((<2>3F)4F)5G
	-	255492.0	-	96% 3d8 4s 4p ((<2>1G)2G)3H
	257799.0	257730.0	69.0	97% 3d9 4f 3H
	-	280419.0	-	100% 3d9 5f 3H

Table III.

HF and LSF parameters of even configurations of Zn III in Cm^{-1}

1 system 1 sigma(4)= 287.00 CONVERGED.

configuration	parameter	LSF	accuracy	HF	LSF/HF
3d10	E0(3d10)	2994.8	290.0	3089.9	
3d9 4s	E0(3d9 4s)	80175.3	148.0	71785.5	1.124
	zeta(3d)	1171.0	141.0	1083.7	1.081
	G2(3d, 4s)	8112.5	92.0	11221.5	0.723
3d9 5s	E0(3d9 5s)	216219.9	155.0	205840.6	1.052
	zeta(3d)	1091.6	(fixed)	1091.7	1.000
	G2(3d, 5s)	1719.5	19.0	2378.5	0.723
3d9 6s	E0(3d9 6s)	251280.1	(fixed)	251271.8	1.000
	zeta(3d)	1093.2	(fixed)	1093.2	1.000
	G2(3d, 6s)	698.4	(fixed)	931.2	0.750
3d9 7s	E0(3d9 7s)	272311.1	(fixed)	272308.5	1.000
	zeta(3d)	1093.7	(fixed)	1093.7	1.000
	G2(3d, 7s)	349.8	(fixed)	466.4	0.750
3d9 8s	E0(3d9 8s)	283806.4	(fixed)	283798.0	1.000
	zeta(3d)	1093.9	(fixed)	1093.9	1.000
	G2(3d, 8s)	200.7	(fixed)	267.7	0.750
3d9 9s	E0(3d9 9s)	290777.0	(fixed)	290777.3	1.000
	zeta(3d)	1094.0	(fixed)	1094.1	1.000
	G2(3d, 9s)	126.0	(fixed)	168.1	0.750
3d9 4d	E0(3d9 4d)	218624.0	75.0	206828.2	1.058
	zeta(3d)	1091.8	(fixed)	1091.8	1.000
	zeta(4d)	39.2	(fixed)	39.2	1.000
	F2(3d, 4d)	6663.5	75.0	8132.9	0.819
	F4(3d, 4d)	2535.0	29.0	3094.1	0.819
	G0(3d, 4d)	2132.9	24.0	2950.3	0.723
	G2(3d, 4d)	2033.0	23.0	2812.2	0.723
	G4(3d, 4d)	1449.4	16.0	2004.9	0.723
3d9 5d	E0(3d9 5d)	252224.6	(fixed)	252215.6	1.000
	zeta(3d)	1093.1	(fixed)	1093.2	1.000
	zeta(5d)	17.3	(fixed)	17.4	0.994
	F2(3d, 5d)	2659.4	(fixed)	3128.8	0.850
	F4(3d, 5d)	1074.1	(fixed)	1263.7	0.850
	G0(3d, 5d)	913.3	(fixed)	1217.8	0.750
	G2(3d, 5d)	898.3	(fixed)	1197.9	0.750
	G4(3d, 5d)	647.5	(fixed)	863.4	0.750
3d9 6d	E0(3d9 6d)	272873.7	(fixed)	272868.1	1.000
	zeta(3d)	1093.6	(fixed)	1093.7	1.000
	zeta(6d)	9.2	(fixed)	9.2	1.000
	F2(3d, 6d)	1332.5	(fixed)	1567.7	0.850
	F4(3d, 6d)	554.6	(fixed)	652.5	0.850
	G0(3d, 6d)	469.3	(fixed)	625.8	0.750
	G2(3d, 6d)	468.2	(fixed)	624.3	0.750
	G4(3d, 6d)	339.1	(fixed)	452.2	0.750
3d9 5g	E0(3d9 5g)	270772.2	(fixed)	270772.1	1.000
	zeta(3d)	1094.2	(fixed)	1094.2	1.000
	zeta(5g)	0.1	(fixed)	0.1	1.000
	F2(3d, 5g)	378.9	(fixed)	445.8	0.850
	F4(3d, 5g)	24.3	(fixed)	28.7	0.847
	G2(3d, 5g)	1.9	(fixed)	2.6	0.731
	G4(3d, 5g)	1.2	(fixed)	1.7	0.706

		G6(3d, 5g)	0.9	(fixed)	1.2	0.750
	3d9 6g	E0(3d9 6g)	282866.0	(fixed)	282865.2	1.000
		zeta(3d)	1094.2	(fixed)	1094.2	1.000
		zeta(6g)	0.0	(fixed)	0.1	0.000
		F2(3d, 6g)	220.3	(fixed)	259.2	0.850
		F4(3d, 6g)	17.9	(fixed)	21.1	0.848
		G2(3d, 6g)	2.0	(fixed)	2.7	0.741
		G4(3d, 6g)	1.3	(fixed)	1.8	0.722
		G6(3d, 6g)	0.9	(fixed)	1.3	0.692
	3d9 7g	E0(3d9 7g)	290167.4	(fixed)	290162.7	1.000
		zeta(3d)	1094.2	(fixed)	1094.3	1.000
		zeta(7g)	0.0	(fixed)	0.0	
		F2(3d, 7g)	138.9	(fixed)	163.5	0.850
		F4(3d, 7g)	12.6	(fixed)	14.9	0.846
		G2(3d, 7g)	1.6	(fixed)	2.2	0.727
		G4(3d, 7g)	1.0	(fixed)	1.4	0.714
		G6(3d, 7g)	0.7	(fixed)	1.1	0.636
	3d9 8g	E0(3d9 8g)	294908.2	(fixed)	294903.4	1.000
		zeta(3d)	1094.2	(fixed)	1094.3	1.000
		zeta(8g)	0.0	(fixed)	0.0	
		F2(3d, 8g)	93.1	(fixed)	109.5	0.850
		F4(3d, 8g)	9.0	(fixed)	10.7	0.841
		G2(3d, 8g)	1.2	(fixed)	1.7	0.706
		G4(3d, 8g)	0.8	(fixed)	1.1	0.727
		G6(3d, 8g)	0.6	(fixed)	0.8	0.750
	3d8 4s2	E0(3d8 4s2)	204654.6	113.0	193495.1	1.059
		F2(3d, 3d)	100196.9	1134.0	122290.8	0.819
		F4(3d, 3d)	62719.6	710.0	76549.6	0.819
		alfa(3d)	0.0	(fixed)		
		beta(3d)	0.0	(fixed)		
		T(3d)	0.0	(fixed)		
		zeta(3d)	1168.1	(fixed)	1168.1	1.000
3d10	-3d9 4s	R2(3d, 3d; 3d, 4s)	-652.1	(fixed)	-869.5	0.750
3d10	-3d9 5s	R2(3d, 3d; 3d, 5s)	0.1	(fixed)	0.2	0.500
3d10	-3d9 6s	R2(3d, 3d; 3d, 6s)	43.7	(fixed)	58.3	0.750
3d10	-3d9 7s	R2(3d, 3d; 3d, 7s)	43.0	(fixed)	57.4	0.749
3d10	-3d9 8s	R2(3d, 3d; 3d, 8s)	37.3	(fixed)	49.7	0.751
3d10	-3d9 9s	R2(3d, 3d; 3d, 9s)	31.7	(fixed)	42.3	0.749
3d10	-3d9 4d	R0(3d, 3d; 3d, 4d)	1250.2	(fixed)	1666.9	0.750
		R2(3d, 3d; 3d, 4d)	9048.7	(fixed)	12065.0	0.750
		R4(3d, 3d; 3d, 4d)	6155.7	(fixed)	8207.6	0.750
3d10	-3d9 5d	R0(3d, 3d; 3d, 5d)	785.6	(fixed)	1047.4	0.750
		R2(3d, 3d; 3d, 5d)	5663.7	(fixed)	7551.6	0.750
		R4(3d, 3d; 3d, 5d)	3863.7	(fixed)	5151.6	0.750
3d10	-3d9 6d	R0(3d, 3d; 3d, 6d)	557.1	(fixed)	742.8	0.750
		R2(3d, 3d; 3d, 6d)	4009.7	(fixed)	5346.3	0.750
		R4(3d, 3d; 3d, 6d)	2738.3	(fixed)	3651.1	0.750
3d10	-3d9 5g	R2(3d, 3d; 3d, 5g)	152.1	(fixed)	202.8	0.750
		R4(3d, 3d; 3d, 5g)	66.3	(fixed)	88.3	0.751
3d10	-3d9 6g	R2(3d, 3d; 3d, 6g)	156.9	(fixed)	209.2	0.750
		R4(3d, 3d; 3d, 6g)	68.9	(fixed)	91.9	0.750
3d10	-3d9 7g	R2(3d, 3d; 3d, 7g)	143.5	(fixed)	191.3	0.750
		R4(3d, 3d; 3d, 7g)	63.4	(fixed)	84.5	0.750
3d10	-3d9 8g	R2(3d, 3d; 3d, 8g)	127.4	(fixed)	169.9	0.750
		R4(3d, 3d; 3d, 8g)	56.4	(fixed)	75.3	0.749
3d10	-3d8 4s2	R2(3d, 3d; 4s, 4s)	10835.3	(fixed)	14447.1	0.750
3d9 4s	-3d9 5s	R0(3d, 4s; 3d, 5s)	377.2	(fixed)	503.0	0.750
		R2(3d, 4s; 5s, 3d)	3762.0	(fixed)	5016.1	0.750
3d9 4s	-3d9 6s	R0(3d, 4s; 3d, 6s)	232.6	(fixed)	310.1	0.750
		R2(3d, 4s; 6s, 3d)	2317.3	(fixed)	3089.7	0.750
3d9 4s	-3d9 7s	R0(3d, 4s; 3d, 7s)	163.4	(fixed)	217.9	0.750
		R2(3d, 4s; 7s, 3d)	1627.4	(fixed)	2169.9	0.750
3d9 4s	-3d9 8s	R0(3d, 4s; 3d, 8s)	123.3	(fixed)	164.4	0.750
		R2(3d, 4s; 8s, 3d)	1227.6	(fixed)	1636.8	0.750
3d9 4s	-3d9 9s	R0(3d, 4s; 3d, 9s)	97.4	(fixed)	129.9	0.750
		R2(3d, 4s; 9s, 3d)	970.1	(fixed)	1293.4	0.750
3d9 4s	-3d9 4d	R2(3d, 4s; 3d, 4d)	8310.7	(fixed)	11081.0	0.750

		R2(3d, 4s; 4d, 3d)	2826.9	(fixed)	3769.1	0.750
3d9 4s	-3d9 5d	R2(3d, 4s; 3d, 5d)	5362.7	(fixed)	7150.3	0.750
		R2(3d, 4s; 5d, 3d)	1943.4	(fixed)	2591.1	0.750
3d9 4s	-3d9 6d	R2(3d, 4s; 3d, 6d)	3851.9	(fixed)	5135.8	0.750
		R2(3d, 4s; 6d, 3d)	1431.6	(fixed)	1908.9	0.750
3d9 4s	-3d9 5g	R4(3d, 4s; 3d, 5g)	-125.2	(fixed)	-166.9	0.750
		R2(3d, 4s; 5g, 3d)	-90.9	(fixed)	-121.2	0.750
3d9 4s	-3d9 6g	R4(3d, 4s; 3d, 6g)	-127.7	(fixed)	-170.3	0.750
		R2(3d, 4s; 6g, 3d)	-93.2	(fixed)	-124.3	0.750
3d9 4s	-3d9 7g	R4(3d, 4s; 3d, 7g)	-116.1	(fixed)	-154.8	0.750
		R2(3d, 4s; 7g, 3d)	-84.9	(fixed)	-113.2	0.750
3d9 4s	-3d9 8g	R4(3d, 4s; 3d, 8g)	-102.6	(fixed)	-136.8	0.750
		R2(3d, 4s; 8g, 3d)	-75.2	(fixed)	-100.3	0.750
3d9 4s	-3d8 4s2	R2(3d, 3d; 3d, 4s)	1083.7	(fixed)	1444.9	0.750
3d9 5s	-3d9 6s	R0(3d, 5s; 3d, 6s)	0.0	(fixed)	0.0	
		R2(3d, 5s; 6s, 3d)	1114.2	(fixed)	1485.6	0.750
3d9 5s	-3d9 7s	R0(3d, 5s; 3d, 7s)	0.0	(fixed)	0.0	
		R2(3d, 5s; 7s, 3d)	787.1	(fixed)	1049.4	0.750
3d9 5s	-3d9 8s	R0(3d, 5s; 3d, 8s)	0.0	(fixed)	0.0	
		R2(3d, 5s; 8s, 3d)	595.5	(fixed)	794.0	0.750
3d9 5s	-3d9 9s	R0(3d, 5s; 3d, 9s)	0.0	(fixed)	0.0	
		R2(3d, 5s; 9s, 3d)	471.4	(fixed)	628.6	0.750
3d9 5s	-3d9 4d	R2(3d, 5s; 3d, 4d)	1215.6	(fixed)	1620.7	0.750
		R2(3d, 5s; 4d, 3d)	1206.1	(fixed)	1608.1	0.750
3d9 5s	-3d9 5d	R2(3d, 5s; 3d, 5d)	1740.8	(fixed)	2321.0	0.750
		R2(3d, 5s; 5d, 3d)	844.1	(fixed)	1125.5	0.750
3d9 5s	-3d9 6d	R2(3d, 5s; 3d, 6d)	1403.7	(fixed)	1871.6	0.750
		R2(3d, 5s; 6d, 3d)	626.5	(fixed)	835.3	0.750
3d9 5s	-3d9 5g	R4(3d, 5s; 3d, 5g)	15.4	(fixed)	20.6	0.748
		R2(3d, 5s; 5g, 3d)	-31.2	(fixed)	-41.6	0.750
3d9 5s	-3d9 6g	R4(3d, 5s; 3d, 6g)	9.9	(fixed)	13.1	0.756
		R2(3d, 5s; 6g, 3d)	-32.2	(fixed)	-43.0	0.749
3d9 5s	-3d9 7g	R4(3d, 5s; 3d, 7g)	6.1	(fixed)	8.1	0.753
		R2(3d, 5s; 7g, 3d)	-29.5	(fixed)	-39.3	0.751
3d9 5s	-3d9 8g	R4(3d, 5s; 3d, 8g)	3.8	(fixed)	5.1	0.745
		R2(3d, 5s; 8g, 3d)	-26.2	(fixed)	-34.9	0.751
3d9 6s	-3d9 7s	R0(3d, 6s; 3d, 7s)	0.0	(fixed)	0.0	
		R2(3d, 6s; 7s, 3d)	494.1	(fixed)	658.8	0.750
3d9 6s	-3d9 8s	R0(3d, 6s; 3d, 8s)	0.0	(fixed)	0.0	
		R2(3d, 6s; 8s, 3d)	374.2	(fixed)	498.9	0.750
3d9 6s	-3d9 9s	R0(3d, 6s; 3d, 9s)	0.0	(fixed)	0.0	
		R2(3d, 6s; 9s, 3d)	296.4	(fixed)	395.1	0.750
3d9 6s	-3d9 4d	R2(3d, 6s; 3d, 4d)	760.0	(fixed)	1013.4	0.750
		R2(3d, 6s; 4d, 3d)	733.5	(fixed)	978.0	0.750
3d9 6s	-3d9 5d	R2(3d, 6s; 3d, 5d)	621.2	(fixed)	828.3	0.750
		R2(3d, 6s; 5d, 3d)	515.4	(fixed)	687.2	0.750
3d9 6s	-3d9 6d	R2(3d, 6s; 3d, 6d)	661.8	(fixed)	882.4	0.750
		R2(3d, 6s; 6d, 3d)	383.2	(fixed)	510.9	0.750
3d9 6s	-3d9 5g	R4(3d, 6s; 3d, 5g)	-0.1	(fixed)	-0.2	0.500
		R2(3d, 6s; 5g, 3d)	-17.9	(fixed)	-23.9	0.749
3d9 6s	-3d9 6g	R4(3d, 6s; 3d, 6g)	1.3	(fixed)	1.7	0.765
		R2(3d, 6s; 6g, 3d)	-18.5	(fixed)	-24.7	0.749
3d9 6s	-3d9 7g	R4(3d, 6s; 3d, 7g)	1.3	(fixed)	1.7	0.765
		R2(3d, 6s; 7g, 3d)	-17.0	(fixed)	-22.6	0.752
3d9 6s	-3d9 8g	R4(3d, 6s; 3d, 8g)	1.1	(fixed)	1.4	0.786
		R2(3d, 6s; 8g, 3d)	-15.1	(fixed)	-20.1	0.751
3d9 7s	-3d9 8s	R0(3d, 7s; 3d, 8s)	0.0	(fixed)	0.0	
		R2(3d, 7s; 8s, 3d)	265.0	(fixed)	353.3	0.750
3d9 7s	-3d9 9s	R0(3d, 7s; 3d, 9s)	0.0	(fixed)	0.0	
		R2(3d, 7s; 9s, 3d)	209.9	(fixed)	279.9	0.750
3d9 7s	-3d9 4d	R2(3d, 7s; 3d, 4d)	525.0	(fixed)	700.0	0.750
		R2(3d, 7s; 4d, 3d)	512.2	(fixed)	682.9	0.750
3d9 7s	-3d9 5d	R2(3d, 7s; 3d, 5d)	436.8	(fixed)	582.4	0.750
		R2(3d, 7s; 5d, 3d)	360.5	(fixed)	480.6	0.750
3d9 7s	-3d9 6d	R2(3d, 7s; 3d, 6d)	349.3	(fixed)	465.7	0.750
		R2(3d, 7s; 6d, 3d)	268.2	(fixed)	357.6	0.750
3d9 7s	-3d9 5g	R4(3d, 7s; 3d, 5g)	-0.1	(fixed)	-0.1	1.000
		R2(3d, 7s; 5g, 3d)	-12.2	(fixed)	-16.3	0.748
3d9 7s	-3d9 6g	R4(3d, 7s; 3d, 6g)	-0.2	(fixed)	-0.3	0.667
		R2(3d, 7s; 6g, 3d)	-12.6	(fixed)	-16.8	0.750
3d9 7s	-3d9 7g	R4(3d, 7s; 3d, 7g)	0.0	(fixed)	-0.1	0.000

		R2(3d, 7s; 7g, 3d)	-11.6	(fixed)	-15.4	0.753
3d9 7s	-3d9 9g	R4(3d, 7s; 3d, 8g)	0.0	(fixed)	0.0	
		R2(3d, 7s; 8g, 3d)	-10.3	(fixed)	-13.7	0.752
3d9 8s	-3d9 9s	R0(3d, 8s; 3d, 9s)	0.0	(fixed)	0.0	
		R2(3d, 8s; 9s, 3d)	159.1	(fixed)	212.1	0.750
3d9 8s	-3d9 4d	R2(3d, 8s; 3d, 4d)	391.8	(fixed)	522.4	0.750
		R2(3d, 8s; 4d, 3d)	385.2	(fixed)	513.6	0.750
3d9 8s	-3d9 5d	R2(3d, 8s; 3d, 5d)	325.0	(fixed)	433.3	0.750
		R2(3d, 8s; 5d, 3d)	271.3	(fixed)	361.7	0.750
3d9 8s	-3d9 6d	R2(3d, 8s; 3d, 6d)	263.1	(fixed)	350.7	0.750
		R2(3d, 8s; 6d, 3d)	201.9	(fixed)	269.2	0.750
3d9 8s	-3d9 5g	R4(3d, 8s; 3d, 5g)	-0.1	(fixed)	-0.1	1.000
		R2(3d, 8s; 5g, 3d)	-9.0	(fixed)	-12.1	0.744
3d9 8s	-3d9 6g	R4(3d, 8s; 3d, 6g)	-0.2	(fixed)	-0.2	1.000
		R2(3d, 8s; 6g, 3d)	-9.4	(fixed)	-12.5	0.752
3d9 8s	-3d9 7g	R4(3d, 8s; 3d, 7g)	-0.2	(fixed)	-0.3	0.667
		R2(3d, 8s; 7g, 3d)	-8.6	(fixed)	-11.5	0.748
3d9 8s	-3d9 8g	R4(3d, 8s; 3d, 8g)	-0.2	(fixed)	-0.3	0.667
		R2(3d, 8s; 8g, 3d)	-7.6	(fixed)	-10.2	0.745
3d9 9s	-3d9 4d	R2(3d, 9s; 3d, 4d)	307.5	(fixed)	410.0	0.750
		R2(3d, 9s; 4d, 3d)	303.8	(fixed)	405.1	0.750
3d9 9s	-3d9 5d	R2(3d, 9s; 3d, 5d)	254.4	(fixed)	339.2	0.750
		R2(3d, 9s; 5d, 3d)	214.1	(fixed)	285.5	0.750
3d9 9s	-3d9 6d	R2(3d, 9s; 3d, 6d)	205.7	(fixed)	274.3	0.750
		R2(3d, 9s; 6d, 3d)	159.4	(fixed)	212.5	0.750
3d9 9s	-3d9 5g	R4(3d, 9s; 3d, 5g)	-0.1	(fixed)	-0.1	1.000
		R2(3d, 9s; 5g, 3d)	-7.1	(fixed)	-9.4	0.755
3d9 9s	-3d9 6g	R4(3d, 9s; 3d, 6g)	-0.2	(fixed)	-0.2	1.000
		R2(3d, 9s; 6g, 3d)	-7.3	(fixed)	-9.8	0.745
3d9 9s	-3d9 7g	R4(3d, 9s; 3d, 7g)	-0.2	(fixed)	-0.3	0.667
		R2(3d, 9s; 7g, 3d)	-6.7	(fixed)	-9.0	0.744
3d9 9s	-3d9 8g	R4(3d, 9s; 3d, 8g)	-0.2	(fixed)	-0.3	0.667
		R2(3d, 9s; 8g, 3d)	-6.0	(fixed)	-8.0	0.750
3d9 4d	-3d9 5d	R0(3d, 4d; 3d, 5d)	0.0	(fixed)	0.0	
		R2(3d, 4d; 3d, 5d)	3223.4	(fixed)	4297.9	0.750
		R4(3d, 4d; 3d, 5d)	1442.0	(fixed)	1922.7	0.750
		R0(3d, 4d; 5d, 3d)	1420.0	(fixed)	1893.3	0.750
		R2(3d, 4d; 5d, 3d)	1373.3	(fixed)	1831.1	0.750
		R4(3d, 4d; 5d, 3d)	984.2	(fixed)	1312.3	0.750
3d9 4d	-3d9 6d	R0(3d, 4d; 3d, 6d)	0.0	(fixed)	0.0	
		R2(3d, 4d; 3d, 6d)	2178.9	(fixed)	2905.2	0.750
		R4(3d, 4d; 3d, 6d)	1021.0	(fixed)	1361.4	0.750
		R0(3d, 4d; 6d, 3d)	1016.8	(fixed)	1355.7	0.750
		R2(3d, 4d; 6d, 3d)	989.0	(fixed)	1318.7	0.750
		R4(3d, 4d; 6d, 3d)	710.3	(fixed)	947.1	0.750
3d9 4d	-3d9 5g	R2(3d, 4d; 3d, 5g)	-596.2	(fixed)	-794.9	0.750
		R4(3d, 4d; 3d, 5g)	-93.6	(fixed)	-124.7	0.751
		R2(3d, 4d; 5g, 3d)	-22.1	(fixed)	-29.4	0.752
		R4(3d, 4d; 5g, 3d)	-17.4	(fixed)	-23.2	0.750
3d9 4d	-3d9 6g	R2(3d, 4d; 3d, 6g)	-545.1	(fixed)	-726.8	0.750
		R4(3d, 4d; 3d, 6g)	-91.3	(fixed)	-121.8	0.750
		R2(3d, 4d; 6g, 3d)	-22.3	(fixed)	-29.8	0.748
		R4(3d, 4d; 6g, 3d)	-17.7	(fixed)	-23.6	0.750
3d9 4d	-3d9 7g	R2(3d, 4d; 3d, 7g)	-466.1	(fixed)	-621.4	0.750
		R4(3d, 4d; 3d, 7g)	-80.9	(fixed)	-107.9	0.750
		R2(3d, 4d; 7g, 3d)	-20.2	(fixed)	-26.9	0.751
		R4(3d, 4d; 7g, 3d)	-16.1	(fixed)	-21.5	0.749
3d9 4d	-3d9 8g	R2(3d, 4d; 3d, 8g)	-396.7	(fixed)	-529.0	0.750
		R4(3d, 4d; 3d, 8g)	-70.4	(fixed)	-93.9	0.750
		R2(3d, 4d; 8g, 3d)	-17.8	(fixed)	-23.7	0.751
		R4(3d, 4d; 8g, 3d)	-14.2	(fixed)	-19.0	0.747
3d9 4d	-3d8 4s2	R2(3d, 4d; 4s, 4s)	-5781.8	(fixed)	-7709.0	0.750
3d9 5d	-3d9 6d	R0(3d, 5d; 3d, 6d)	0.0	(fixed)	0.0	
		R2(3d, 5d; 3d, 6d)	1557.8	(fixed)	2077.1	0.750
		R4(3d, 5d; 3d, 6d)	677.8	(fixed)	903.7	0.750
		R0(3d, 5d; 6d, 3d)	654.6	(fixed)	872.8	0.750
		R2(3d, 5d; 6d, 3d)	648.3	(fixed)	864.4	0.750
		R4(3d, 5d; 6d, 3d)	468.4	(fixed)	624.6	0.750
3d9 5d	-3d9 5g	R2(3d, 5d; 3d, 5g)	88.5	(fixed)	118.0	0.750
		R4(3d, 5d; 3d, 5g)	-30.7	(fixed)	-41.0	0.749
		R2(3d, 5d; 5g, 3d)	-14.6	(fixed)	-19.5	0.749

		R4(3d, 5d; 5g, 3d)	-11.4	(fixed)	-15.2	0.750
3d9 5d	-3d9 6g	R2(3d, 5d; 3d, 6g)	-37.0	(fixed)	-49.3	0.751
		R4(3d, 5d; 3d, 6g)	-35.0	(fixed)	-46.7	0.749
		R2(3d, 5d; 6g, 3d)	-14.9	(fixed)	-19.8	0.753
		R4(3d, 5d; 6g, 3d)	-11.7	(fixed)	-15.5	0.755
3d9 5d	-3d9 7g	R2(3d, 5d; 3d, 7g)	-72.3	(fixed)	-96.4	0.750
		R4(3d, 5d; 3d, 7g)	-33.1	(fixed)	-44.2	0.749
		R2(3d, 5d; 7g, 3d)	-13.5	(fixed)	-18.0	0.750
		R4(3d, 5d; 7g, 3d)	-10.6	(fixed)	-14.1	0.752
3d9 5d	-3d9 8g	R2(3d, 5d; 3d, 8g)	-79.7	(fixed)	-106.3	0.750
		R4(3d, 5d; 3d, 8g)	-29.9	(fixed)	-39.8	0.751
		R2(3d, 5d; 8g, 3d)	-11.9	(fixed)	-15.9	0.748
		R4(3d, 5d; 8g, 3d)	-9.4	(fixed)	-12.5	0.752
3d9 5d	-3d8 4s2	R2(3d, 5d; 4s, 4s)	-3544.4	(fixed)	-4725.8	0.750
3d9 6d	-3d9 5g	R2(3d, 6d; 3d, 5g)	-7.7	(fixed)	-10.3	0.748
		R4(3d, 6d; 3d, 5g)	-19.8	(fixed)	-26.4	0.750
		R2(3d, 6d; 5g, 3d)	-10.6	(fixed)	-14.2	0.746
		R4(3d, 6d; 5g, 3d)	-8.2	(fixed)	-11.0	0.745
3d9 6d	-3d9 6g	R2(3d, 6d; 3d, 6g)	28.6	(fixed)	38.2	0.749
		R4(3d, 6d; 3d, 6g)	-21.0	(fixed)	-28.0	0.750
		R2(3d, 6d; 6g, 3d)	-10.8	(fixed)	-14.4	0.750
		R4(3d, 6d; 6g, 3d)	-8.4	(fixed)	-11.2	0.750
3d9 6d	-3d9 7g	R2(3d, 6d; 3d, 7g)	2.6	(fixed)	3.4	0.765
		R4(3d, 6d; 3d, 7g)	-19.9	(fixed)	-26.5	0.751
		R2(3d, 6d; 7g, 3d)	-9.8	(fixed)	-13.1	0.748
		R4(3d, 6d; 7g, 3d)	-7.7	(fixed)	-10.2	0.755
3d9 6d	-3d9 8g	R2(3d, 6d; 3d, 8g)	-10.4	(fixed)	-13.9	0.748
		R4(3d, 6d; 3d, 8g)	-18.0	(fixed)	-24.0	0.750
		R2(3d, 6d; 8g, 3d)	-8.6	(fixed)	-11.5	0.748
		R4(3d, 6d; 8g, 3d)	-6.8	(fixed)	-9.0	0.756
3d9 6d	-3d8 4s2	R2(3d, 6d; 4s, 4s)	-2486.5	(fixed)	-3315.4	0.750
3d9 5g	-3d9 6g	R0(3d, 5g; 3d, 6g)	0.0	(fixed)	0.0	
		R2(3d, 5g; 3d, 6g)	194.9	(fixed)	259.8	0.750
		R4(3d, 5g; 3d, 6g)	17.4	(fixed)	23.2	0.750
		R2(3d, 5g; 6g, 3d)	2.0	(fixed)	2.7	0.741
		R4(3d, 5g; 6g, 3d)	1.3	(fixed)	1.7	0.765
		R6(3d, 5g; 6g, 3d)	0.9	(fixed)	1.3	0.692
3d9 5g	-3d9 7g	R0(3d, 5g; 3d, 7g)	0.0	(fixed)	0.0	
		R2(3d, 5g; 3d, 7g)	138.1	(fixed)	184.1	0.750
		R4(3d, 5g; 3d, 7g)	14.1	(fixed)	18.8	0.750
		R2(3d, 5g; 7g, 3d)	1.8	(fixed)	2.4	0.750
		R4(3d, 5g; 7g, 3d)	1.2	(fixed)	1.6	0.750
		R6(3d, 5g; 7g, 3d)	0.9	(fixed)	1.1	0.818
3d9 5g	-3d9 8g	R0(3d, 5g; 3d, 8g)	0.0	(fixed)	0.0	
		R2(3d, 5g; 3d, 8g)	105.9	(fixed)	141.2	0.750
		R4(3d, 5g; 3d, 8g)	11.7	(fixed)	15.5	0.755
		R2(3d, 5g; 8g, 3d)	1.6	(fixed)	2.1	0.762
		R4(3d, 5g; 8g, 3d)	1.0	(fixed)	1.4	0.714
		R6(3d, 5g; 8g, 3d)	0.8	(fixed)	1.0	0.800
3d9 6g	-3d9 7g	R0(3d, 6g; 3d, 7g)	0.0	(fixed)	0.0	
		R2(3d, 6g; 3d, 7g)	137.0	(fixed)	182.7	0.750
		R4(3d, 6g; 3d, 7g)	13.1	(fixed)	17.5	0.749
		R2(3d, 6g; 7g, 3d)	1.8	(fixed)	2.4	0.750
		R4(3d, 6g; 7g, 3d)	1.2	(fixed)	1.6	0.750
		R6(3d, 6g; 7g, 3d)	0.9	(fixed)	1.2	0.750
3d9 6g	-3d9 8g	R0(3d, 6g; 3d, 8g)	0.0	(fixed)	0.0	
		R2(3d, 6g; 3d, 8g)	105.6	(fixed)	140.8	0.750
		R4(3d, 6g; 3d, 8g)	11.0	(fixed)	14.6	0.753
		R2(3d, 6g; 8g, 3d)	1.6	(fixed)	2.2	0.727
		R4(3d, 6g; 8g, 3d)	1.1	(fixed)	1.4	0.786
		R6(3d, 6g; 8g, 3d)	0.8	(fixed)	1.0	0.800
3d9 7g	-3d9 8g	R0(3d, 7g; 3d, 8g)	0.0	(fixed)	0.0	
		R2(3d, 7g; 3d, 8g)	93.9	(fixed)	125.3	0.749
		R4(3d, 7g; 3d, 8g)	9.4	(fixed)	12.6	0.746
		R2(3d, 7g; 8g, 3d)	1.5	(fixed)	2.0	0.750
		R4(3d, 7g; 8g, 3d)	1.0	(fixed)	1.3	0.769
		R6(3d, 7g; 8g, 3d)	0.7	(fixed)	0.9	0.778

Table IV.

HF and LSF parameters of odd configurations of Zn III in Cm^{-1} :

1 system 2 sigma(5)= 264.00 CONVERGED.

configuration		parameter	LSF	accuracy	HF	LSF/HF
3d9 4p		E0(3d9 4p)	143735.6	81.0	133348.1	1.080
		zeta(3d)	1140.4	88.0	1087.2	1.049
		zeta(4p)	1010.8	154.0	889.9	1.136
		F2(3d, 4p)	17915.2	572.0	19300.0	0.928
		G1(3d, 4p)	6298.4	282.0	7055.6	0.891
		G3(3d, 4p)	5385.4	241.0	6042.5	0.891
3d9 5p		E0(3d9 5p)	235900.9	110.0	225450.6	1.047
		zeta(3d)	1130.2	90.0	1092.2	1.035
		zeta(5p)	405.1	254.0	290.1	1.396
		F2(3d, 5p)	4779.5	651.0	5468.0	0.874
		G1(3d, 5p)	1655.1	74.0	1854.9	0.891
		G3(3d, 5p)	1509.3	68.0	1693.5	0.891
3d9 6p		E0(3d9 6p)	269953.2	122.0	259952.0	1.039
		zeta(3d)	403.8	99.0	1093.3	0.369
		zeta(6p)	132.1	(fixed)	132.1	1.000
		F2(3d, 6p)	571.0	924.0	2336.6	0.244
		G1(3d, 6p)	707.1	32.0	793.4	0.891
		G3(3d, 6p)	657.2	29.0	737.3	0.891
3d9 4f		E0(3d9 4f)	258947.9	83.0	247606.6	1.047
		zeta(3d)	1115.1	67.0	1094.2	1.019
		zeta(4f)	0.3	(fixed)	0.3	1.000
		F2(3d, 4f)	1719.4	(fixed)	2022.9	0.850
		F4(3d, 4f)	0.0	2557.0	370.6	0.000
		G1(3d, 4f)	225.1	10.0	252.6	0.891
		G3(3d, 4f)	127.4	6.0	143.0	0.891
		G5(3d, 4f)	73.1	(fixed)	97.5	0.750
3d9 5f		E0(3d9 5f)	281602.8	278.0	270300.3	1.043
		zeta(3d)	1094.1	(fixed)	1094.2	1.000
		zeta(5f)	0.1	(fixed)	0.2	0.500
		F2(3d, 5f)	873.9	(fixed)	1028.2	0.850
		F4(3d, 5f)	193.0	(fixed)	227.1	0.850
		G1(3d, 5f)	167.2	7.0	187.7	0.891
		G3(3d, 5f)	95.1	4.0	106.7	0.891
		G5(3d, 5f)	65.6	3.0	72.9	0.892
3d8 4s 4p		E0(3d8 4s 4p)	250535.9	(fixed)	250536.6	1.000
		F2(3d, 3d)	104235.5	(fixed)	122630.1	0.850
		F4(3d, 3d)	65263.6	(fixed)	76780.8	0.850
		alfa(3d)	0.0	(fixed)		
		beta(3d)	0.0	(fixed)		
		T(3d)	0.0	(fixed)		
		zeta(3d)	1170.9	(fixed)	1171.0	1.000
		zeta(4p)	1095.9	(fixed)	1095.9	1.000
		F2(3d, 4p)	18044.8	(fixed)	21229.2	0.850
		G2(3d, 4s)	8470.0	(fixed)	11293.4	0.750
		G1(3d, 4p)	5546.8	(fixed)	7395.8	0.750
		G3(3d, 4p)	4903.0	(fixed)	6537.4	0.750
		G1(4s, 4p)	43657.7	(fixed)	58210.3	0.750
3d9 4p	-3d9 5p	R0(3d, 4p; 3d, 5p)	0.0	(fixed)	0.0	
		R2(3d, 4p; 3d, 5p)	6104.5	(fixed)	8139.3	0.750
		R1(3d, 4p; 5p, 3d)	2671.4	(fixed)	3561.8	0.750
		R3(3d, 4p; 5p, 3d)	2367.0	(fixed)	3156.0	0.750
3d9 4p	-3d9 6p	R0(3d, 4p; 3d, 6p)	0.0	(fixed)	0.0	
		R2(3d, 4p; 3d, 6p)	3781.4	(fixed)	5041.8	0.750
		R1(3d, 4p; 6p, 3d)	1731.0	(fixed)	2308.0	0.750
		R3(3d, 4p; 6p, 3d)	1547.8	(fixed)	2063.7	0.750

3d9 4p	-3d9 4f	R2(3d, 4p; 3d, 4f)	2849.7	(fixed)	3799.5	0.750
		R4(3d, 4p; 3d, 4f)	875.7	(fixed)	1167.6	0.750
		R1(3d, 4p; 4f, 3d)	661.7	(fixed)	882.2	0.750
		R3(3d, 4p; 4f, 3d)	465.1	(fixed)	620.1	0.750
3d9 4p	-3d9 5f	R2(3d, 4p; 3d, 5f)	2281.7	(fixed)	3042.3	0.750
		R4(3d, 4p; 3d, 5f)	736.4	(fixed)	981.9	0.750
		R1(3d, 4p; 5f, 3d)	563.2	(fixed)	750.9	0.750
		R3(3d, 4p; 5f, 3d)	400.2	(fixed)	533.6	0.750
3d9 4p	-3d8 4s 4p	R2(3d, 3d; 3d, 4s)	1241.5	(fixed)	1655.3	0.750
		R2(3d, 4p; 4s, 4p)	-11141.4	(fixed)	-14855.2	0.750
		R1(3d, 4p; 4p, 4s)	-11341.0	(fixed)	-15121.4	0.750
3d9 5p	-3d9 6p	R0(3d, 5p; 3d, 6p)	0.0	(fixed)	0.0	
		R2(3d, 5p; 3d, 6p)	2446.1	(fixed)	3261.4	0.750
		R1(3d, 5p; 6p, 3d)	908.8	(fixed)	1211.7	0.750
		R3(3d, 5p; 6p, 3d)	837.1	(fixed)	1116.1	0.750
3d9 5p	-3d9 4f	R2(3d, 5p; 3d, 4f)	42.1	(fixed)	56.2	0.749
		R4(3d, 5p; 3d, 4f)	270.9	(fixed)	361.2	0.750
		R1(3d, 5p; 4f, 3d)	305.6	(fixed)	407.4	0.750
		R3(3d, 5p; 4f, 3d)	222.9	(fixed)	297.2	0.750
3d9 5p	-3d9 5f	R2(3d, 5p; 3d, 5f)	427.6	(fixed)	570.1	0.750
		R4(3d, 5p; 3d, 5f)	261.1	(fixed)	348.2	0.750
		R1(3d, 5p; 5f, 3d)	262.4	(fixed)	349.8	0.750
		R3(3d, 5p; 5f, 3d)	193.8	(fixed)	258.3	0.750
3d9 5p	-3d8 4s 4p	R2(3d, 3d; 3d, 4s)	0.0	(fixed)	0.0	
		R2(3d, 5p; 4s, 4p)	-3781.3	(fixed)	-5041.7	0.750
		R1(3d, 5p; 4p, 4s)	-3825.7	(fixed)	-5100.9	0.750
3d9 6p	-3d9 4f	R2(3d, 6p; 3d, 4f)	139.6	(fixed)	186.1	0.750
		R4(3d, 6p; 3d, 4f)	162.1	(fixed)	216.2	0.750
		R1(3d, 6p; 4f, 3d)	192.8	(fixed)	257.0	0.750
		R3(3d, 6p; 4f, 3d)	142.0	(fixed)	189.3	0.750
3d9 6p	-3d9 5f	R2(3d, 6p; 3d, 5f)	79.3	(fixed)	105.7	0.750
		R4(3d, 6p; 3d, 5f)	149.9	(fixed)	199.9	0.750
		R1(3d, 6p; 5f, 3d)	165.9	(fixed)	221.2	0.750
		R3(3d, 6p; 5f, 3d)	123.7	(fixed)	165.0	0.750
3d9 6p	-3d8 4s 4p	R2(3d, 3d; 3d, 4s)	0.0	(fixed)	0.0	
		R2(3d, 6p; 4s, 4p)	-2152.6	(fixed)	-2870.1	0.750
		R1(3d, 6p; 4p, 4s)	-2169.3	(fixed)	-2892.4	0.750
3d9 4f	-3d9 5f	R0(3d, 4f; 3d, 5f)	0.0	(fixed)	0.0	
		R2(3d, 4f; 3d, 5f)	885.3	(fixed)	1180.4	0.750
		R4(3d, 4f; 3d, 5f)	209.9	(fixed)	279.8	0.750
		R1(3d, 4f; 5f, 3d)	163.2	(fixed)	217.6	0.750
		R3(3d, 4f; 5f, 3d)	92.6	(fixed)	123.4	0.750
		R5(3d, 4f; 5f, 3d)	63.2	(fixed)	84.3	0.750
3d9 4f	-3d8 4s 4p	R2(3d, 4f; 4s, 4p)	-3089.3	(fixed)	-4119.0	0.750
		R3(3d, 4f; 4p, 4s)	-1856.4	(fixed)	-2475.2	0.750
3d9 5f	-3d8 4s 4p	R2(3d, 5f; 4s, 4p)	-2463.8	(fixed)	-3285.1	0.750
		R3(3d, 5f; 4p, 4s)	-1539.3	(fixed)	-2052.4	0.750

Table V: Zn III Observed wavelengths and their corresponding transitions [16].

Observed Wavelengths (Å) of Zn III	Corresponding Transitions	Level energy (Cm^{-1})
1869.9473	$3d^9 4d$-$3d^9 6p$	218909.40-272406.00
1942.9709	$3d^9 4d$-$3d^8 4s(2P)4p$	221343.60-272818.00
1982.1207	$3d^9 4d$-$3d^8 4s(2D)4p$	217073.80-267514.00
2033.9146	$3d^8 4s^2$-$3d^8 4s(4P)$ 4p	211920.70-261090.00
2087.3915	$3d^9 4d$-$3d^8 4s(2D)4p$	218041.50-265955.00
2163.4539	$3d^9 4d$-$3d^9 4f$	214357.00-260584.10
2246.0916	$3d^9 4d$-$3d^9 4f$	216464.50-260981.90
2252.5723	$3d^9 4d$-$3d^8 4s(2D)4p$	221143.70-265531.00
2271.2040	$3d^9 4d$-$3d^8 4s(4P)4p$	217073.80-261090.00
2282.4148	$3d^9 4d$-$3d^8 4s(4P)4p$	216895.30-260710.00
2286.3870	$3d^9 4d$-$3d^8 4s(2D)4p$	221343.60-265088.00
2290.2114	$3d^9 4d$-$3d^8 4s(2D)4p$	221343.60-264998.00
2333.9546	$3d^8 4s^2$-$3d^9 5p$	192763.70-235623.90

References

1. G. Milazzo and G. Cecchetti, Applied Spectroscopy, Vol. **23**, Issue 3, pp. 197-203 (1969).
2. G. Milazzo, "Vacuum Ultra-Violet Spectroscopy", Pure Appl. Chem., Vol. 4, No. 1, pp. 135-140 (1962).
3. B. H. Bransden and C.J. Joachain, "Physics of atoms and molecules", Pearson Education India, (2003).
4. D. Fluri, ETH Zurich, "Molecular Universe", Atomic Spectroscopy, p.2, HS (2009).
5. Robert D. Cowan, "The Theory of Atomic Structure and Spectra", (University of California Press, Berkeley, 1981), esp. Chapters 8 and 16.
6. R. A. Sawyer, "Experimental Spectroscopy", Prentice-Hall, Inc., New York (1951).
7. J. A. R. Samson, "Techniques of Vacuum Ultra Violet Spectroscopy", John Wiley and Sons, Inc. (1967).
8. CH. Palmer and E. Loewen, "Diffraction Grating Handbook", 6th edition, Newport Corporation (2005).
9. G. R. Harrison, "Practical Spectroscopy", Prentice-Hall, Inc., Englewood Cliffs, N.J. (1948).
10. Hilger and Watts, Ltd., J. Sci. Instrum., Vol. 30, p.438, (1953).
11. Hilger and Watts, Ltd., J. Sci. Instrum., Vol. 35, p.187, (1958).
12. K. M. Varier, "Advanced Experimental Techniques in Modern Physics", Pragati Prakashan, 1st edition, (2006).
13. D. S. Mathur, "Mechanics", S. Chand & Company LTD (1981).
14. R. O. Hutchinson, "Arc and Spark Spectra of Aluminum, Zinc, and Carbon in the Extreme Ultra-Violet", Astrophysical Journal, vol. 58, p.280 (1923).
15. J. G VAN HET HOF, A computer program "Mosfit2" for wavelength calibration using a polynomial fit. (Private communication)
16. Atomic Line List v2.04, http://www.pa.uky.edu/~peter/atomic/
17. R. A. Sawyer, "The Vacuum Hot-Spark Spectrum of Zinc in the Extreme Ultra-Violet Region", Astrophysical Journal, vol. 52, p.286 (1920).

18. Laporte, O., and Lang, R. J., Phys. Rev. Vol. 30, p.378, (1927).
19. J. Sugar and A. Musgrove, J. Phys. Chem. Ref. Data. Vol.24, No. 6, p.1803-1872, (1995).
20. http://users.ipfw.edu/masters/Im2Spec/Im2Spec.html
21. C. Lengacher, S. Macklin, D. Hite, and M. F. Masters, Am. J. Phys., Vol. 66, No. 11, p.1025-1028, (1998).